

Alignment and Comparison of Directed Networks via Transition Couplings of Random Walks

Bongsoo Yi*

Department of Statistics and Operations Research,
University of North Carolina at Chapel Hill, Chapel Hill, North Carolina, USA

Kevin O'Connor*

Department of Statistics and Operations Research,
University of North Carolina at Chapel Hill, Chapel Hill, North Carolina, USA

Kevin McGoff

Department of Mathematics and Statistics,
University of North Carolina at Charlotte, Charlotte, North Carolina, USA

Andrew B. Nobel†

Department of Statistics and Operations Research,
University of North Carolina at Chapel Hill, Chapel Hill, North Carolina, USA

Abstract

We describe and study a transport based procedure called NetOTC (network optimal transition coupling) for the comparison and alignment of two networks. The networks of interest may be directed or undirected, weighted or unweighted, and may have distinct vertex sets of different sizes. Given two networks and a cost function relating their vertices, NetOTC finds a transition coupling of their associated random walks having minimum expected cost. The minimizing cost quantifies the difference between the networks, while the optimal transport plan itself provides alignments of both the vertices and the edges of the two networks. Coupling of the full random walks, rather than their marginal distributions, ensures that NetOTC captures local and global information about the networks, and preserves edges. NetOTC has no free parameters, and does not rely on randomization. We investigate a number of theoretical properties of NetOTC and present experiments establishing its empirical performance.

Keywords: graph alignment, graph comparison, graph factor, optimal transport

*Bongsoo Yi and Kevin O'Connor are co-first authors for the paper.

†Corresponding author; E-mail: nobel@email.unc.edu

1 Introduction

Networks have long been used as a means of representing and studying the pairwise interactions between a set of individuals or objects under study. More recently, networks themselves have become objects of study, including exploratory analysis and statistical modeling. When an application of interest involves multiple networks, analysis often begins with the problem of network alignment or comparison, tasks that have been studied in a number of fields. Network alignment compares and finds correspondences among nodes or edges within multiple networks. The aim is to recognize similar substructures, unveiling hidden relationships and functional similarities that exist within different networks. In the simplest version of the network alignment problem, one is given two networks with vertex sets of equal size and seeks to find a bijection between the vertex sets that maximizes the number of aligned edges. Numerous approaches to network alignment have been considered in the literature, e.g. Kelley *et al.* (2003); Kuchaiev *et al.* (2010); Kuchaiev and Przulj (2011); Kalaev *et al.* (2008); Klau (2009). By contrast, the goal of network comparison is more general: given two networks of different size or structure, identify and quantify similarities between them in a rigorous manner. Perhaps the simplest form of comparison is a numerical measure of similarity between networks, which one might hope to have the properties of a metric. Potentially more informative measures of comparison include soft alignment of vertices and edges in the two networks.

Network alignment and comparison arise in a number of disciplines where network models are common. In biology, networks have been used to represent protein-protein interactions and gene regulatory systems. Network alignment has been used to identify interaction structures and topological similarities, facilitating the transfer of biological insights from familiar to unexplored species (Singh *et al.*, 2008; Elmsallati *et al.*, 2016; Ma and Liao, 2020). In connectomics and neuroimaging, networks are used to model connectivity and interactions of different brain regions. Network alignment and comparison methods have been used to compare the connectomes of healthy and diseased individuals (Zalesky *et al.*, 2010; Milano *et al.*, 2017) as an initial step in identifying potential indicators of disease, understanding disease origins, and identifying specific locations within the brain that could influence the progression or onset of the disease. Beyond biology and neuroscience, network comparison methods have found applications in economics (Fagiolo *et al.*, 2010; Engel *et al.*, 2021), where they have been used to compare trade networks over time, and to identify shifts and trends in economic dynamics. In social science, comparisons of social networks have offered insights into the relationships and interactions between different groups (Jackson *et al.*, 2014; Mislove *et al.*, 2007).

In this paper, we propose and analyze NetOTC, a procedure for the comparison and soft alignment of two networks. The networks of interest may be directed or undirected, weighted or unweighted, and may have distinct vertex sets of different sizes. NetOTC, which is short for network optimal transition coupling, is based on applying a process-level optimal transport method to the random walks arising from each network. In more detail, the NetOTC procedure takes as input two connected networks G_1 and G_2 with non-negative edge weights, which may be directed or undirected, and a cost function relating their vertices. Each network gives rise to a stationary random walk on its vertex set whose transition probabilities are determined by normalizing the edge weights at each node. NetOTC proceeds by finding a joint chain on the product of the vertex sets of G_1 and G_2 that has the following properties: the joint chain is stationary and Markov; the joint chain minimizes the expected value of the cost function at any fixed time point; and the transition distribution from each state (u, v) in the joint chain is obtained by coupling the transition distribution of u in G_1 with the transition distribution of v in G_2 . The latter condition, which gives rise to transition couplings, ensures that the joint chain is a coupling of the initial chains on the individual graphs. More information about process couplings and transition couplings can be found in Section 3. We note that minimization of the expected cost subject to the constraints given above is carried out analytically, and not through Monte Carlo methods.

As described above, the optimal transport plan arising from NetOTC is a stationary random walk on the product of the given networks that favors low cost pairs of vertices, while maintaining the marginal structure of the random walks on each individual network. The cost function used in NetOTC is specified by the user, and will, in general, be application dependent. Cost functions can be based, for example, on the difference between externally specified vertex attributes, the distance between Euclidean embeddings of the vertices, or the difference between the degrees of the vertices. If the given networks have the same vertex set, a cost function based on vertex identity may be used as well.

The NetOTC procedure has a number of desirable methodological and theoretical properties. On the methodological side, NetOTC applies to directed and undirected networks, and readily handles networks with different sizes and connectivity structures. NetOTC has no free parameters and does not make use of randomization or Monte Carlo techniques. As NetOTC considers process-level couplings of random walks, the optimal transport plan captures global information reflected in the stationary distributions of the random walks, as well as local information that is present in the transition probabilities between vertices. The expected cost of the optimal transport plan provides a numerical measure of the difference between the networks. The distribution of the optimal transport

plan at a single time point yields a soft, probabilistic alignment of the vertices in the given networks. Moreover, the distribution of the optimal transport plan at two successive time points yields a soft, probabilistic alignment of the *edges* of the given networks. To the best of our knowledge, native alignment of edges is unique to NetOTC among existing alignment and comparison methods. Once the vertex cost function has been specified, the exact version of the NetOTC procedure has no free parameters and does not make use of randomization.

On the theoretical side, we establish several key properties of the NetOTC procedure that support its use in comparison and alignment tasks. The edge alignment of NetOTC respects edges, in the sense that vertex pairs in the given networks are aligned with positive probability only if each pair is connected by an edge in its respective network. Although the NetOTC optimal transport plan minimizes the expected cost between vertices at time zero, stationarity ensures that the same is true at any other fixed time, and that the coupled random walk has a low average cost between vertices across time. The NetOTC similarity measure is sensitive to differences in the k -step behavior of the random walks on G_1 and G_2 if these differences affect the cumulative cost. For undirected networks with a common vertex set, the NetOTC similarity is a metric on equivalence classes of networks having identical random walks if the cost c is a metric. For the zero-one cost, the NetOTC similarity is lower bounded by the ℓ_1 -difference of the network degree sequences, and the ℓ_1 -difference of the network weight functions.

In addition, we study the structure of the NetOTC method through network factors. Our definition of factor, which arises naturally when considering functions of Markov chains, differs from other definitions in the network theory literature. Informally, a network G_2 is a factor of a network G_1 if the vertices of G_2 can be associated, via a vertex map f , with disjoint sets of vertices in G_1 between which aggregate weights can be consistently defined. We show that if G_2 is a factor of G_1 , then the vertex map f yields a deterministic transition coupling of their associated random walks. Under suitable compatibility conditions on the cost function, this coupling will be optimal and will provide a solution to the NetOTC problem. The resulting expected cost, vertex alignment, and edge alignment are fully determined by the structure of G_1 and the map f . Importantly, the existence and precise nature of the map f need not be known to the NetOTC procedure. These results extend to paired factors: an optimal transition coupling for a pair of networks can be mapped in a deterministic fashion to an optimal transition coupling of their factors when the cost functions for each pair are compatible with the factor maps.

As a complement to the theory, we carry out a number of simulations and numerical experiments to assess the performance of NetOTC and compare it with other optimal transport-based comparison methods in the literature. NetOTC is competitive with other methods on a number of network classification tasks. In an extensive experiment on pairs of isomorphic networks with small to moderate sizes, NetOTC was consistently able to recover the isomorphism using a local (degree-based) cost function, substantially outperforming other methods. When applied to stochastic block models (with equivalent blocks of different sizes) using a degree-based cost function, NetOTC was competitive with other methods in its ability to align vertices in equivalent blocks, and substantially better at aligning edges. We also considered the problem of comparing a network to an exact or approximate factor using a distance-based cost derived from Euclidean vertex embeddings of the given networks. NetOTC outperforms other methods in its ability to align vertices in the parent and factor networks. While the performance gap is modest for exact factors, it increases as one considers approximate factors.

1.1 Outline of the Paper

The next section gives an overview of existing work on optimal transport and related approaches to network comparison and alignment. Section 3 provides background concerning random walks on directed networks, optimal transport for Markov chains, and transition couplings. The NetOTC procedure is described in Section 4, including computation, the optimal transport cost, and vertex and edge alignment. Section 5 is devoted to the formal statement and discussion of the theoretical properties of NetOTC. Proofs are given in Section 8. Section 6 contains a number of simulations and a number of experiments that demonstrate the flexibility and potential utility of NetOTC. Additional details concerning the experiments are given in Appendix A.

2 Related Work

The problems of network alignment and comparison have received a lot of recent attention in the literature. Approaches using optimal transport ideas can be divided into several groups: spectral methods, variants of Gromov-Wasserstein, and methods involving random walks and Markov chains. Other approaches make use of quadratic programming and continuous approximations. This related work is discussed below.

Spectral Methods. One line of work (Dong and Sawin, 2020; Maretic *et al.*, 2019, 2020) uses techniques from spectral graph theory to define optimal transport (OT) problems for networks. In particular, this approach associates

to each network a multivariate Gaussian with zero mean and covariance matrix equal to the pseudo-inverse of the graph Laplacian. The Wasserstein distance between Gaussian distributions of the same dimension may be computed analytically in terms of their respective covariance matrices. For networks with different numbers of vertices, Margetic *et al.* (2020) and Dong and Sawin (2020) propose to optimize this distance over soft many-to-one assignments between vertices in either network. At present, this family of approaches is unable to incorporate available feature information or underlying cost functions, relying only on their intrinsic structure.

Variants of Gromov-Wasserstein. Another line of work (Mémoli, 2011; Peyré *et al.*, 2016; Titouan *et al.*, 2019; Vayer *et al.*, 2019, 2020) considers the Gromov-Wasserstein (GW) distance and related extensions. In this work, one tries to couple distributions on the vertices in each network so as to minimize an expected transport cost between vertices while minimizing changes in edges between the two networks. This approach allows one to capture differences in both features and structure between networks. We refer the reader to Dong and Sawin (2020) for a discussion on the differences between spectral-based network OT methods and GW distances. A number of variants of the GW distance have been proposed for a variety of tasks including cross-domain alignment (Chen *et al.*, 2020), graph partitioning (Xu *et al.*, 2019a), graph matching (Xu *et al.*, 2019a,b), and node embedding (Xu *et al.*, 2019b). The work (Barbe *et al.*, 2020) proposes to incorporate global structure into the Wasserstein and Fused GW (FGW) distances by applying heat diffusion to the vertex features before computing the cost matrix.

Methods involving random walks and Markov chains. It is well-known that a weighted network G with non-negative edge weights can be viewed as a Markov chain $X = \{X_k\}_{k=1}^\infty$, and there is previous work that uses this perspective to align or compare networks. The paper (Vishwanathan *et al.*, 2010) studies a flexible family of kernels for comparing two given networks. Given networks G and H with associated transition matrices P and Q the kernels take the form $\kappa(G, H) = \sum_{k \geq 1} \mu_k q^t (P \otimes Q)^k p$, where p and q are starting and stopping distributions, μ_k are non-negative weights, and $(P \otimes Q)^k$ is the k -step transition matrix of the independent coupling of the random walks on G and H . The free parameters $p, q, \{\mu_k\}$ are user specified; appropriate choices allow for efficient computation. The kernels $\kappa(G, H)$ are distinct from NetOTC, as they employ only independent couplings, and do not involve the use of optimal transport.

Several recent papers (Chen *et al.*, 2022, 2023) have studied a Markov chain-based distance function for networks that has close connections to the classical Weisfeiler-Lehman (WL) test for graph isomorphism. Given two weighted networks G and H and a fixed time $k \geq 1$, the k -step WL-distance $d_{\text{WL}}^k(G, H)$ is equal to the minimum expected cost $\min \mathbb{E}c(\tilde{X}_k, \tilde{Y}_k)$ at time k , where the minimum is taken over all (possibly time-inhomogeneous) Markovian couplings of X and Y . The transition couplings used in the present work have the additional requirement that they must be time-homogeneous and stationary (see Section 3.3). The family $\{d_{\text{WL}}^k : k \geq 1\}$ is further investigated in (Brugere *et al.*, 2023), where it is shown (in Proposition 23) that

$$d_{\text{WL}}^\infty(G, H) := \lim_k d_{\text{WL}}^k(G, H) = \sup_k d_{\text{WL}}^k(G, H). \quad (1)$$

Moreover, it is shown in Proposition 5 of (Brugere *et al.*, 2023) that

$$d_{\text{WL}}^\infty(G, H) \leq d_{\text{OTC}}(G, H), \quad (2)$$

where d_{OTC} is the NetOTC distance studied in this paper. Using (1) and (2) one may verify that the k -step WL-distance is not in general equal to d_{OTC} . Furthermore, (2) ensures that the NetOTC distance has at least as much discriminatory power as the WL-test in the graph isomorphism detection problem. We refer the reader to Brugere *et al.* (2023) for more details.

Lastly, let us mention that there is a constrained optimal transport method called Causal Optimal Transport (COT) that has been used in finance and machine learning (Lassalle, 2013). By Lemma 3.11 in Chen *et al.* (2023), any Markovian coupling is also a bi-causal coupling, and therefore the transition couplings considered in this paper are also bi-causal. However, Theorem 3.12 from Chen *et al.* (2023) states that the k -step WL distance is equal to the bi-causal transport distance in which the given cost function is evaluated at time k . Thus, the relationship between the OTC distance and COT is the same as the relationship between OTC and the WL-distances: they are distinct notions, with d_{OTC} greater than or equal to bi-causal transport distance at any fixed time.

Other Methods for Network Alignment and Comparison. There is also a large body of work devoted to network alignment and comparison that does not use optimal transport methods. The network alignment problem can be generally defined as a quadratic programming problem under discrete and doubly stochastic constraints (Yan *et al.*, 2016; Jiang *et al.*, 2017; Loiola *et al.*, 2007; Cho *et al.*, 2010; Cour *et al.*, 2007). However, as the optimal network alignment problem is well known to be an NP-hard problem (Garey and Johnson, 1990), it is

computationally challenging to obtain an optimal alignment for networks. For this reason, many authors have proposed approximate solutions for network alignment (Cho *et al.*, 2010; Zhou and De la Torre, 2016; Yu *et al.*, 2018; Enqvist *et al.*, 2009; van Wyk and van Wyk, 2004; Zaslavskiy *et al.*, 2009). Among these approximate methods, most of the successful algorithms start with relaxing the discrete constraints to create a continuous condition. Several authors (Schellewald and Schnörr, 2005; Torr, 2003) relax the discrete conditions to form a positive semi-definite problem. A non-convex quadratic programming problem was adopted in Gold and Rangarajan (1996); Cho *et al.* (2010); Zhou and De la Torre (2016). In another direction, Leordeanu and Hebert (2005) introduces spectral matching as a simple relaxation, and Cour *et al.* (2007) strengthens this approach by giving an affine constraint. Also, Jiang *et al.* (2017) proposes an algorithm that can efficiently solve a general quadratic programming problem with doubly stochastic constraints. Each step of the algorithm is easy to implement and the convergence is guaranteed. Generally, after finding the optimal solution for the relaxed continuous problem, the discrete alignment is attained through a final discretization process (Cho *et al.*, 2010; Leordeanu and Hebert, 2005; Leordeanu *et al.*, 2009). We note that these approaches may find a solution that is locally optimal but not globally optimal.

Another line of research is devoted to the statistical and probabilistic analysis of graph matching when the given graphs are generated at random but are correlated with one another, e.g., each is a random perturbation of a given graph (Ding *et al.*, 2020; Barak *et al.*, 2019; Cullina *et al.*, 2020; Cullina and Kiyavash, 2017; Feizi *et al.*, 2020; Korula and Lattanzi, 2014; Lyzinski *et al.*, 2014; Yartseva and Grossglauser, 2013). Much of this work investigates various matching procedures under specific random graph models, such as correlated Erdos-Renyi graphs, and is concerned with the information-theoretic threshold for exact recovery, and the time complexity of the matching procedures.

3 Transition Couplings of Random Walks on Networks

This section provides background for the detailed description of the NetOTC procedure. We begin by recalling how a weighted network gives rise to a random walk on its vertex set and reviewing the definition and framework of optimal transport. We then consider transition couplings of random walks, which preserve stationarity and the Markov property. The computation of optimal transition couplings is the basis for the NetOTC procedure, which is described in Section 4 below.

3.1 Random Walks on Directed Networks

Let $G = (U, E, w)$ denote a network with finite vertex set U , edge set $E \subseteq U \times U$, and non-negative weight function $w : U \times U \rightarrow \mathbb{R}_+$. An ordered pair $(u, u') \in E$ represents a directed edge from u to u' with weight $w(u, u')$. We assume in what follows that $w(u, u') > 0$ if and only if $(u, u') \in E$. For any vertex $u \in U$, we let $d(u) = \sum_{u' \in U} w(u, u')$ be the weighted out-degree of u . An undirected network is represented by a directed network in which $w(u, u') = w(u', u)$ for each $u, u' \in U$. A path in G is an ordered sequence of vertices $u_0, \dots, u_n \in U$ such that $(u_{i-1}, u_i) \in E$ for each $i = 1, \dots, n$. A network G is strongly connected if for each ordered pair $(u, v) \in U \times U$ there exists a path u_0, \dots, u_n in G such that $u_0 = u$ and $u_n = v$. In this case $d(u) > 0$ for each vertex $u \in U$.

To any network $G = (U, E, w)$, one may associate a Markov transition kernel $P(\cdot | \cdot)$ with state space U as follows: for each pair of vertices u and u' , the probability of transitioning from u to u' is

$$P(u' | u) = \frac{w(u, u')}{d(u)}. \quad (3)$$

Recall that a probability distribution p on U is said to be stationary for $P(\cdot | \cdot)$ if $p(u') = \sum_{u \in U} p(u) P(u' | u)$ for all $u' \in U$. It follows from the Perron-Frobenius theorem that the transition kernel $P(\cdot | \cdot)$ admits at least one stationary distribution p . Together, P and p define a stationary Markov chain $X = X_0, X_1, X_2, \dots \in U$ such that for any u_0, \dots, u_n in U

$$\mathbb{P}(X_0 = u_0, \dots, X_n = u_n) = p(u_0) \prod_{i=0}^{n-1} P(u_{i+1} | u_i).$$

The Markov chain X is commonly referred to as a random walk on G . When G is strongly connected, the kernel $P(\cdot | \cdot)$ admits a *unique* stationary distribution, and we refer to X as *the* random walk on G . Random walks on networks have been studied extensively in the probability literature, and have found numerous applications in fields ranging from genomics to computer science, including recent work on network embedding (Hamilton, 2020;

Grover and Leskovec, 2016; Perozzi *et al.*, 2014). In what follows, we will generally assume that the networks under consideration are strongly connected. In this case, the random walk X on G is an irreducible Markov chain (Chapter 4 of Blum *et al.* (2020)).

3.2 Optimal Transport

Let X and Y be random objects taking values in sets \mathcal{X} and \mathcal{Y} , respectively. In what follows we are primarily interested in the case that X and Y are processes. A *coupling* of X and Y is a jointly distributed pair (\tilde{X}, \tilde{Y}) of random objects taking values in $\mathcal{X} \times \mathcal{Y}$ with the property that $\tilde{X} \stackrel{d}{=} X$ and $\tilde{Y} \stackrel{d}{=} Y$. Here $\tilde{X} \stackrel{d}{=} X$ means that \tilde{X} and X have the same distribution on \mathcal{X} , and $\tilde{Y} \stackrel{d}{=} Y$ is interpreted similarly. The distinction between X, Y and \tilde{X}, \tilde{Y} arises from the fact that X and Y are understood and specified through their individual distributions, whereas \tilde{X} and \tilde{Y} are understood and specified as a jointly distributed pair. (In general, X and Y may be defined on different probability spaces, whereas \tilde{X} and \tilde{Y} are necessarily defined on the same probability space.) Couplings have been widely studied in the probability literature, and are the basic objects of interest in optimal transport.

Let $\Pi(X, Y)$ denote the set of all couplings (\tilde{X}, \tilde{Y}) of X and Y . Note that $\Pi(X, Y)$ is not empty, as it always contains the independent coupling (\tilde{X}, \tilde{Y}) in which \tilde{X} and \tilde{Y} are independent copies of X and Y , respectively. Each coupling $(\tilde{X}, \tilde{Y}) \in \Pi(X, Y)$ is associated with a joint distribution π on $(\mathcal{X} \times \mathcal{Y}, \mathcal{A} \times \mathcal{B})$ that can be viewed conditionally as a plan for transporting the distribution of X to that of Y and vice versa. Let $c : \mathcal{X} \times \mathcal{Y} \rightarrow \mathbb{R}_+$ be a measurable, non-negative cost function relating the elements of \mathcal{X} and \mathcal{Y} . The optimal transport problem is to minimize the expected value of the cost function over all couplings of X and Y , namely

$$\text{minimize } \mathbb{E}c(\tilde{X}, \tilde{Y}) \text{ over } (\tilde{X}, \tilde{Y}) \in \Pi(X, Y).$$

A minimizer of the optimal transport problem is called an optimal coupling of X and Y , or an optimal transport plan. The theory and applications of optimal transport are active areas of research. See Peyré and Cuturi (2019); Villani (2008) for further reading and more details.

3.3 Transition Couplings

Let $G_1 = (U, E_1, w_1)$ and $G_2 = (V, E_2, w_2)$ be weighted directed networks, and let $c : U \times V \rightarrow \mathbb{R}_+$ be a cost function relating their vertex sets. As described above, the network G_1 is associated with a random walk $X = X_0, X_1, \dots$ on the vertex set U . We may regard the process X as a random element of the set $\mathcal{X} = U^{\mathbb{N}}$ equipped with the Borel sigma-field arising from the usual product topology on $U^{\mathbb{N}}$. Similarly, the network G_2 is associated with a random walk $Y = Y_0, Y_1, \dots$ taking values in $\mathcal{Y} = V^{\mathbb{N}}$. A coupling of the processes X and Y is a joint process

$$(\tilde{X}, \tilde{Y}) = (\tilde{X}_0, \tilde{Y}_0), (\tilde{X}_1, \tilde{Y}_1), (\tilde{X}_2, \tilde{Y}_2), \dots$$

with values in $U \times V$ such that $\tilde{X} = \tilde{X}_0, \tilde{X}_1, \dots \stackrel{d}{=} X$ and $\tilde{Y} = \tilde{Y}_0, \tilde{Y}_1, \dots \stackrel{d}{=} Y$, where $\stackrel{d}{=}$ indicates equality of distribution. In general, a coupling of X and Y need not be stationary or Markov, an issue that we take up below.

In studying optimal transport of the random walks X and Y we make use of the single letter cost $\tilde{c} : \mathcal{X} \times \mathcal{Y} \rightarrow \mathbb{R}$ defined by $\tilde{c}(x, y) = c(x_0, y_0)$. The standard optimal transport problem with the cost \tilde{c} seeks to minimize $\mathbb{E}c(\tilde{X}_0, \tilde{Y}_0)$ over the family $\Pi(X, Y)$ of all couplings of the Markov chains X and Y . However, for most purposes $\Pi(X, Y)$ is too large: in general, it will include couplings that are non-stationary, and not Markov of any order. Without further restrictions, an optimal coupling will minimize the expected cost only at time zero, after which the processes \tilde{X} and \tilde{Y} may evolve independently (and potentially have a large realized cost). Restricting attention to stationary couplings addresses some of these issues (O'Connor *et al.*, 2022). We note that stationary couplings of stationary processes, also known as joinings, have been widely studied in the ergodic theory literature (see De La Rue (2005); Glasner (2003); Ornstein (1973) and the references therein).

When considering random walks X and Y on graphs, which are Markov chains, it is natural to consider couplings (\tilde{X}, \tilde{Y}) that are themselves Markov chains, so that the structure of the couplings matches that of the walks. Unfortunately, even the family of stationary first order Markov couplings presents some difficulties: there is no fast method for computing optimal couplings, and the optimal expected cost need not have the properties of a metric even when the cost c does (Ellis, 1976, 1978). For these reasons, we restrict attention to the subfamily of transition couplings, which are defined below.

Definition 1. Let X be a stationary Markov chain with values in U and transition kernel P , and let Y be a stationary Markov chain with values in V and transition kernel Q . A stationary Markov chain (\tilde{X}, \tilde{Y}) with values

in $U \times V$ is a transition coupling of X and Y if it is a coupling of X and Y and if it has a transition kernel R such that for every $u_0, u_1 \in U$ and $v_0, v_1 \in V$,

$$\sum_{v \in V} R(u_1, v | u_0, v_0) = P(u_1 | u_0) \quad \text{and} \quad \sum_{u \in U} R(u, v_1 | u_0, v_0) = Q(v_1 | v_0). \quad (4)$$

Let $\Pi_{\text{TC}}(X, Y)$ denote the set of all transition couplings of X and Y . When (4) holds, we will also say that R is a transition coupling of P and Q .

The transition coupling condition (4) can be stated equivalently as follows: for every state $(u_0, v_0) \in U \times V$ of the joint chain, the distribution $R(\cdot | u_0, v_0)$ of the next state is a coupling of the next state distributions $P(\cdot | u_0)$ and $Q(\cdot | v_0)$ of the individual chains. The set of transition couplings $\Pi_{\text{TC}}(X, Y)$ is non-empty, as the independent coupling of X and Y , with transition kernel $R(u', v' | u, v) = P(u' | u) Q(v' | v)$, is a transition coupling.

Couplings have long been employed in the analysis of Markov chains, often to study the rate at which the marginal distribution of a chain started from a particular state converges to the stationary distribution of the chain. In a typical analysis, two versions of a chain are run from different initial conditions until they reach the same state, after which they coincide. The transition couplings considered here are couplings of two distinct processes, one for each of the given networks. Transition couplings as defined in Definition 1 are sometimes called Markovian couplings in the probability literature (Levin and Peres, 2017), but the use of this terminology is not standardized. The term transition coupling that is used here was introduced in O'Connor *et al.* (2022). Chen *et al.* (2023) use the term Markovian coupling to refer to the class of time-inhomogeneous (non-stationary) Markov couplings in which transition probabilities may vary from time point to time point, and for which the initial distribution is a coupling of the initial distribution of the given processes.

4 NetOTC

In this section, we describe the NetOTC procedure in more detail, including a statement of the NetOTC problem, as well as exact and approximate computational methods for its solution.

4.1 The NetOTC Problem

Let G_1 and G_2 be strongly connected networks of interest. Each network gives rise to a unique random walk on its vertex set, whose transition probabilities are determined by their connectivity and edge weights; the stationary distribution of the walk reflects the global structure of the network, while the transition probabilities of the walk reflect the local structure of the network. Let X and Y be the walks associated with G_1 and G_2 , respectively. In the NetOTC problem, we seek to minimize the expected cost $\mathbb{E}c(\tilde{X}_0, \tilde{Y}_0)$ over all transition couplings (\tilde{X}, \tilde{Y}) of X and Y . In particular, we wish to identify both the minimizing value

$$\rho(G_1, G_2) = \min_{(\tilde{X}, \tilde{Y}) \in \Pi_{\text{TC}}(X, Y)} \mathbb{E}c(\tilde{X}_0, \tilde{Y}_0), \quad (5)$$

and an associated optimal transition coupling

$$(X^*, Y^*) \in \operatorname{argmin}_{(\tilde{X}, \tilde{Y}) \in \Pi_{\text{TC}}(X, Y)} \mathbb{E}c(\tilde{X}_0, \tilde{Y}_0). \quad (6)$$

An optimal transition coupling is a stationary random walk

$$(X^*, Y^*) = (X_0^*, Y_0^*), (X_1^*, Y_1^*), \dots$$

on the product $U \times V$ that preserves the marginal behavior of the walks X and Y , while favoring pairs u, v with low cost. In particular, (X^*, Y^*) is an optimal coupling of the *processes* X and Y , not just their one-dimensional (stationary) distributions. As such, the optimal transport plan identified by NetOTC captures and links the local and global structure of the given networks.

As noted above, the set $\Pi_{\text{TC}}(X, Y)$ of transition couplings is non-empty. We endow $\Pi_{\text{TC}}(X, Y)$ with the standard topology (inherited as a subset of the weak* topology on the space of finite-valued stochastic processes) under which it is compact and the expected cost function $(\tilde{X}_0, \tilde{Y}_0) \mapsto \mathbb{E}c(\tilde{X}_0, \tilde{Y}_0)$ is continuous. Thus, the minimum in (5) is achieved, and there exists an optimal transition coupling in (6). In general, there may be many solutions to the NetOTC problem. For example, if the cost function is constant, then all transition couplings are optimal.

Workflow 1 Solving the NetOTC Problem

Input: Networks $G_1 = (U, E_1, w_1)$ and $G_2 = (V, E_2, w_2)$. Cost function $c(u, v)$.

Step 1. Compute the transition probabilities P and Q of the random walks associated with G_1 and G_2 according to (3)

Step 2. Pass P and Q to the procedure of O'Connor *et al.* (2022), which yields the optimal cost ρ , as well as the stationary distribution π and transition kernel R of an optimal transition coupling

Step 3. Calculate vertex alignment as in (7) and edge alignment as in (8) .

Output: NetOTC cost ρ , Vertex alignment π_v , Edge alignment π_e

While the objective function of the NetOTC problem involves only the first time point of the joint process (\tilde{X}, \tilde{Y}) , the restriction to transition couplings ensures that the optimal coupling performs well on average over multiple time points (see Proposition 4 below), and that it captures the dynamics of the individual chains. In general, the minimizing value of $\mathbb{E}c(\tilde{X}_0, \tilde{Y}_0)$ will (strictly) decrease as one moves from transition couplings to general Markov couplings, from Markov couplings to stationary couplings, and from stationary couplings to general couplings (Ellis, 1976, 1978; Ellis *et al.*, 1980; Ellis, 1980; O'Connor *et al.*, 2022, 2021).

We note that the NetOTC problem is *not* equivalent to the problem of finding a one-step optimal transition coupling, which is considered in (Song *et al.*, 2016; Zhang, 2000). In the latter problem one finds, for every $u \in U$ and $v \in V$, a coupling $(\tilde{X}_0, \tilde{Y}_0)$ of $X_0 \sim P(\cdot|u)$ and $Y_0 \sim Q(\cdot|v)$ minimizing $\mathbb{E}c(\tilde{X}_0, \tilde{Y}_0)$. A one-step optimal transition coupling does not necessarily exhibit good performance over multiple time steps, as it does not account for the global structure of the given networks.

4.2 Cost Functions

In practice, the specification of a cost function depends on the goals of the network alignment or comparison problem. The cost function is typically based on prior information about the vertex sets of the given networks, including vertex features and embeddings, if these are available. If $U = V$ we may use the 0-1 cost $c(u, v) = \mathbb{I}(u \neq v)$. If the vertices of G_1 and G_2 are associated with features or attributes in a common, discrete set \mathcal{S} then one may take $c(u, v) = \rho(\tilde{u}, \tilde{v})$ where ρ is a cost function relating the elements of \mathcal{S} , and $\tilde{u}, \tilde{v} \in \mathcal{S}$ are the features associated with vertices u and v , respectively. If \mathcal{S} is a finite set, the zero-one cost $c(u, v) = \mathbb{I}(\tilde{u} \neq \tilde{v})$ is often a good choice. If the vertices of G_1 and G_2 are embedded in a common Euclidean space \mathbb{R}^d via embeddings $h_1 : U \rightarrow \mathbb{R}^d$ and $h_2 : V \rightarrow \mathbb{R}^d$, then it is natural to use an embedding-based cost such as $c(u, v) = \|h_1(u) - h_2(v)\|$ or $c(u, v) = \|h_1(u) - h_2(v)\|^2$. In cases where such prior maps are unavailable, one may consider costs defined in terms of intrinsic properties of the networks of interest, or embed the vertices in a Euclidean space a priori using methods such as Laplacian eigenmaps (Belkin and Niyogi, 2003).

A cost function that is applicable in general is the degree-based cost: $c(u, v) = (\deg(u) - \deg(v))^2$. For undirected networks, $\deg(u)$ is sum of weights of all edges adjacent to u . For directed networks, one may use in-degree, out-degree, or a combination of these. Unless otherwise specified, we use out-degree in this paper. One may also use the standardized degree $\bar{d}(u) = \deg(u) / \sum_{u' \in U} \deg(u')$ when comparing networks of significantly different sizes. Extending this idea, one may employ cost $c(u, v)$ based on the degree distributions of a fixed local neighborhood of u and v .

4.3 Computation of NetOTCs

A workflow for NetOTC is given in Workflow 1. The NetOTC procedure does not rely on randomization, and has no free parameters: its output is fully determined by the given networks and the cost function c . Finding an optimal transition coupling (OTC) of the random walks X and Y derived from the given networks is a non-convex, constrained optimization problem that is not amenable to standard optimization routines. Instead, NetOTC uses the method of (O'Connor *et al.*, 2022), in which the problem of finding an OTC is reframed as a Markov decision process (MDP) with state space $\mathcal{S} = \mathcal{X} \times \mathcal{Y}$, where the admissible actions in state $s = (x, y)$ correspond to couplings r_s of the transition distributions $P(x, \cdot)$ and $Q(y, \cdot)$. The transition distribution of the MDP in state s with action r_s is simply given by r_s , while the reward function of the MDP is simply the negative of the cost function $R(s, r_s) = -c(x, y)$, where $s = (x, y)$. Reformulated in this way, the OTC problem corresponds to finding an optimal policy for the MDP, a problem to which policy iteration (Howard, 1960) may be applied (with standard optimal transport solvers used in the policy update steps). The algorithm requires $\mathcal{O}((|U||V|)^3)$ operations per iteration. In practice, it converges after fewer than 5 iterations. O'Connor *et al.* (2022) also describes a more efficient

algorithm based on entropic regularization and Sinkhorn iterations. When applied to NetOTC, the regularized algorithm requires $\mathcal{O}((|U||V|)^2)$ operations per iteration (up to poly-logarithmic factors), which is nearly-linear in the dimension of the couplings under consideration, and in this sense comparable to the state-of-the-art for entropic OT algorithms (Peyré and Cuturi, 2019). Pseudocode and more details on the method can be found in Section 4 of O’Connor *et al.* (2022).

In general, NetOTC problem may have multiple solutions. The NetOTC algorithm is only guaranteed to return a single minimizer, which is not guaranteed to be irreducible. On the other hand, the entropically regularized problem has a unique minimizer, which is aperiodic and irreducible when X and Y are aperiodic and irreducible. The current implementation of NetOTC can handle networks with up to 200 vertices. Research on faster computation of OTCs is currently ongoing.

4.4 NetOTC Deliverables

Difference measure for networks. The solution of the NetOTC problem yields the minimizing value $\rho(G_1, G_2)$ of the expected cost, and the associated optimal transition plan (X^*, Y^*) . The minimum cost $\rho(G_1, G_2)$ measures the difference between G_1 and G_2 and can be utilized for network comparison tasks. For undirected networks with the same vertex set, $\rho(\cdot, \cdot)$ is a metric if the cost function is a metric (see Proposition 8).

Vertex alignment. The optimal transport plan (X^*, Y^*) itself provides soft, probabilistic alignments of the vertices and edges of G_1 and G_2 based on the joint distribution of pairs in the coupled chain. The vertex alignment π_v produced by NetOTC is derived from the stationary distribution of the optimal transport plan (X^*, Y^*) , which is the distribution of the pair (X_0^*, Y_0^*) . The vertex alignment is defined by

$$\pi_v(u, v) = \mathbb{P}((X_0^*, Y_0^*) = (u, v)). \quad (7)$$

One may define probabilistic vertex alignments in a similar manner for other OT-based network comparison methods (see Section 6.3 and 6.4).

Edge alignment. A unique feature of NetOTC is that the optimal transport plan naturally yields a probabilistic alignment of the edges of the given networks. The edge alignment is obtained from the first two pairs $\{(X_0^*, Y_0^*), (X_1^*, Y_1^*)\}$ in the optimal transport plan. For $u, u' \in U$ and $v, v' \in V$ the edge alignment is defined by

$$\pi_e((u, u'), (v, v')) = \mathbb{P}((X_0^*, Y_0^*) = (u, v), (X_1^*, Y_1^*) = (u', v')). \quad (8)$$

It is straightforward to show (see Proposition 2) that vertex pairs aligned with positive probability must be adjacent in their respective networks. In other words, NetOTC aligns only existing edges; it does not create new ones. By contrast, most alignment methods in the literature have as their primary focus the matching of vertices, with edges functioning primarily as a means of evaluating matchings. Alignments arising in this way can map adjacent vertices in G_1 to non-adjacent vertices in G_2 , or vice versa.

5 Theoretical Properties of NetOTC

In this section, we explore some theoretical properties of NetOTC, beginning with the edge-alignment property and several results concerning the behavior of NetOTC under average cost criteria. For undirected networks with a common vertex set, we establish that the NetOTC cost has the properties of a metric when the cost c does, and we investigate the sensitivity of NetOTC to local information arising from degree and weight functions. We then define a notion of *network factor* that captures the idea of one network being “folded” or “compressed” to produce another. Although the literature contains several definitions of network factors or factor networks, the definition given here appears to be new. We establish a close connection between factors and transition couplings, and then we present two results describing the behavior of NetOTC in the presence of this type of network factor structure. All proofs of the results in this section may be found in Section 8.

5.1 NetOTC Edge Alignment

The NetOTC edge alignment function π_e respects edges, in the sense that vertex pairs aligned with positive probability must be adjacent in the given networks.

Proposition 2. *Let π_e be the NetOTC edge alignment of networks $G_1 = (U, E_1, w_1)$ and $G_2 = (V, E_2, w_2)$ based on the optimal transport plan (X^*, Y^*) . If $\pi_e((u, u'), (v, v')) > 0$ then $(u, u') \in E_1$ and $(v, v') \in E_2$.*

5.2 NetOTC and Multistep Cost

The NetOTC cost $\rho(G_1, G_2)$ is the expected cost $\mathbb{E}c(\tilde{X}_0, \tilde{Y}_0)$ at the initial state of the optimal transport plan. Stationarity ensures that the NetOTC problem is equivalent to minimizing the long-term average cost over the set of transition couplings.

Definition 3. For an infinite sequence x_0, x_1, \dots and integers $0 \leq i \leq j$ let $x_i^j = (x_i, \dots, x_j)$. For each $k \geq 1$ define the k -step average cost $c_k(x_0^{k-1}, y_0^{k-1}) = k^{-1} \sum_{j=0}^{k-1} c(x_j, y_j)$ and the limiting average cost $\bar{c}(x, y) = \limsup_{k \rightarrow \infty} c_k(x_0^{k-1}, y_0^{k-1})$.

Proposition 4. Let G_1 and G_2 be networks with associated random walks X and Y . Then

$$\rho(G_1, G_2) = \min_{(\tilde{X}, \tilde{Y}) \in \Pi_{\text{TC}}(X, Y)} \mathbb{E}\bar{c}(\tilde{X}, \tilde{Y}),$$

and the optimal transport plans minimizing $\mathbb{E}\bar{c}(\tilde{X}, \tilde{Y})$ coincide with those minimizing $\mathbb{E}c(\tilde{X}_0, \tilde{Y}_0)$.

The long-term behavior of the random walks X and Y encodes information about the global structure of the networks G_1 and G_2 , respectively. The next result shows that NetOTC also captures local information arising from the finite time behavior of the walks X and Y . For example, if G_1 and G_2 are distinguishable based on optimal transport of their k -step random walks, then they are distinguishable by NetOTC.

Proposition 5. Let G_1 and G_2 be networks with associated random walks X and Y . For each $k \geq 1$

$$\rho(G_1, G_2) \geq \min \mathbb{E}c_k(\tilde{X}_0^{k-1}, \tilde{Y}_0^{k-1}),$$

where the minimum is over the family of all couplings of X_0^{k-1} and Y_0^{k-1} .

5.3 Undirected Networks with a Common Vertex Set

In this section, we consider undirected networks $G_1 = (U, E_1, w_1)$ and $G_2 = (U, E_2, w_2)$ with the same vertex set, but potentially different edge sets and weight functions. We assume throughout that the networks are connected. We begin by defining a natural equivalence relation on such networks.

Definition 6. Undirected networks G_1 and G_2 are equivalent, denoted by $G_1 \sim G_2$, if they have the same vertex U , the same edge set E , and there exists a constant $C > 0$ such that $w_1(u, u') = C w_2(u, u')$ for every $u, u' \in U$.

The following result relates the equivalence of networks to their random walks.

Proposition 7. Connected undirected networks G_1 and G_2 are equivalent if and only if their respective random walks are identical.

Whatever the underlying cost c , the cost $\rho(G_1, G_2)$ and optimal transport plan arising from NetOTC depends only on the equivalence classes of the networks G_1 and G_2 . In particular, NetOTC is invariant under (positive) scaling of weight functions. When the underlying cost c is a metric on U , the NetOTC cost is a metric on these equivalence classes.

Proposition 8. If the cost function $c : U \times U \rightarrow \mathbb{R}_+$ satisfies the properties of a metric on U , then ρ is a metric on the equivalence classes of undirected networks with vertex set contained in U defined by \sim .

We now investigate the sensitivity of NetOTC to differences between the degree and weight functions of the given networks.

Definition 9. The degree function of an undirected network $G = (U, E, w)$ is given by $d(u) = \sum_{u' \in U} w(u, u')$ for $u \in U$. Let $D = \sum_{u \in U} d(u)$ denote the total degree of G .

The next proposition strengthens the general result of Proposition 5.

Proposition 10. Let G_1 and G_2 be undirected networks with the same vertex set. Let $d_1(u)$ and $d_2(u)$ be the degree functions of G_1 and G_2 , respectively, and assume that each network has a total degree of D . Then under the zero-one cost $c(u, u') = \mathbb{I}(u \neq u')$,

$$\bullet \quad \rho(G_1, G_2) \geq \frac{1}{2D} \sum_{u \in U} |d_1(u) - d_2(u)|$$

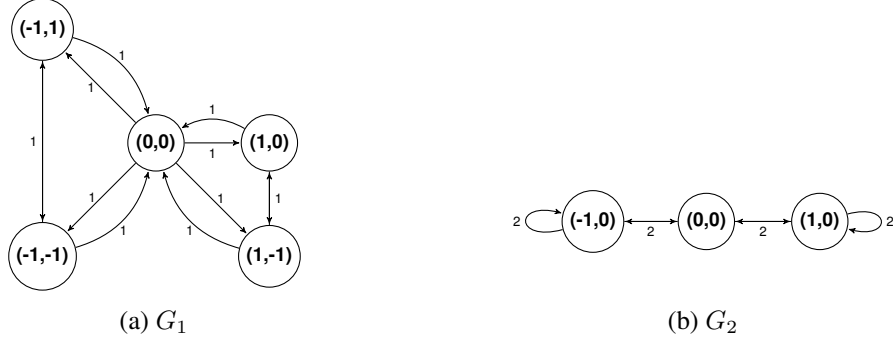


Figure 1: An example of two networks related by a factor map. Here G_2 is a factor of G_1 via the map that collapses vertices along vertical lines.

$$\bullet \rho(G_1, G_2) \geq \frac{1}{4D} \sum_{u, u' \in U} |w_1(u, u') - w_2(u, u')|$$

Remark 11. Proposition 10 can be readily extended to cases where G_1 and G_2 have different total degrees D_1 and D_2 , respectively. Nevertheless, when comparing two undirected networks using NetOTC, we may assume that they share equal total degrees. As indicated in Proposition 7, for a connected undirected network $G_2 = (U, E_2, w_2)$ with total degree D_2 , an equivalent graph $G'_2 = (U, E_2, \frac{D_1}{D_2} w_2)$ with total degree D_1 can be constructed.

5.4 Deterministic Transition Couplings and Factor Maps

The graph theory and network literature contain several definitions of “network factor” and “factor network”. A network factor of G is often defined to be any spanning subnetwork of G , while the term factor network is used in the context of message passing algorithms and error-correcting codes to refer to a bipartite network that captures the factorization of a function or a probability distribution. Here we define a notion of network factor that appears to be different than existing definitions in the literature, see for example the survey (Plummer, 2007). We show that there is a close connection between factors and transition couplings, and we use this to rigorously study the behavior of NetOTC when factor structure is present. Our results establish a close link between NetOTC and factors, behavior that distinguishes NetOTC from other comparison and alignment methods.

Definition 12. Let $G_1 = (U, E_1, w_1)$ and $G_2 = (V, E_2, w_2)$ be strongly connected, weighted directed networks with out-degree functions d_1 and d_2 , respectively. A map $f : U \rightarrow V$ is a factor map if for all $v, v' \in V$ and $u \in f^{-1}(v)$,

$$\sum_{u' \in f^{-1}(v')} w_1(u, u') = \frac{d_1(u)}{d_2(v)} w_2(v, v'). \quad (9)$$

In this case, we will say that G_2 is a factor of G_1 , and that G_1 is an extension of G_2 .

Example 13. Consider the networks G_1 and G_2 drawn in Figure 1 with vertices embedded in \mathbb{R}^2 . G_2 is a factor of G_1 with respect to the map f that takes $(-1, 1)$ and $(-1, -1)$ to $(-1, 0)$, $(0, 0)$ to $(0, 0)$, and $(1, 0)$ and $(1, -1)$ to $(1, 0)$.

The definition of factor arises naturally from the random walk perspective. If G_1 and G_2 have associated random walks X and Y , and G_2 is a factor of G_1 under the map f , then the process $f(X) := f(X_0), f(X_1), \dots$ is equal in distribution to Y , see Theorem 16 below for more details. Factors have been well studied in ergodic theory and symbolic dynamics. The existence of a factor map (in the sense above) ensures that Y is a stationary coding of X , which is a special case of a factor relationship in ergodic theory. Moreover, if G_2 is a factor of G_1 , then the subshift of finite type (SFT) consisting of all bi-infinite walks on G_2 is a topological factor of the SFT associated with G_1 given by a 1-block code (see Lind and Marcus (1995) for detailed definitions). Our definition of factor has points of contact with compressed representations of weighted networks, explored in Toivonen *et al.* (2011), but in general the relationship (9) need not hold for compressed representations.

The definition of factor formalizes the idea that G_2 (the factor) is a collapsed or compressed version of G_1 (the extension). The factor map f associates the vertices in G_2 with a partition of the vertices in G_1 . Condition (9) ensures that the partitioning of the vertices is consistent with the transition probabilities of the random walk on G_1 .

If P and Q are the transition kernels for G_1 and G_2 , then Condition (9) is equivalent to the statement that for all $v, v' \in V$ and $u \in f^{-1}(v)$,

$$\sum_{u' \in f^{-1}(v')} P(u' | u) = Q(v' | v). \quad (10)$$

This is also equivalent to the condition $\mathbb{P}(f(X_1) = v' | X_0 = u) = \mathbb{P}(Y_1 = v' | Y_0 = v)$, where X and Y are the random walks associated with G_1 and G_2 . Since P and Q are irreducible, Condition (9) implies that the (unique) stationary distributions p on G_1 and q on G_2 are such that for all $v \in V$,

$$\sum_{u \in f^{-1}(v)} p(u) = q(v), \quad (11)$$

which is equivalent to $f(X_0) \stackrel{d}{=} Y_0$. The factor relationship can also be expressed in matrix form. If f is a factor map from G_1 to G_2 , then (9) is equivalent to the condition $PF = FQ$ where $F \in \mathbb{R}^{U \times V}$ is defined by $F(u, v) = 1$ if $f(u) = v$ and $F(u, v) = 0$ otherwise. Furthermore equation (11) is equivalent to $pF = q$.

The next proposition establishes a close connection between transition couplings and factor maps. Let G_1 and G_2 be strongly connected, weighted directed networks with associated random walks X and Y . Note that any stationary Markov coupling (\tilde{X}, \tilde{Y}) of X and Y corresponds to a weighted, directed network H with vertex set $W \subset U \times V$. Let $\pi_U : U \times V \rightarrow U$ and $\pi_V : U \times V \rightarrow V$ be the standard projections onto the first and second coordinates, respectively.

Proposition 14. *If (\tilde{X}, \tilde{Y}) is a stationary Markov coupling corresponding to a strongly connected network H with vertex set W , then (\tilde{X}, \tilde{Y}) is a transition coupling of X and Y if and only if the restriction of π_U to W is a factor map from H to G_1 and the restriction of π_V to W is a factor map from H to G_2 .*

We next investigate connections between factors and deterministic transition couplings.

Definition 15. *Suppose $G_1 = (U, E_1, w_1)$ and $G_2 = (V, E_2, w_2)$ are two strongly connected, weighted, directed networks with associated Markov chains X and Y , respectively. A transition coupling (\tilde{X}, \tilde{Y}) is said to be deterministic from X to Y if for each u in U there exists $v \in V$ such that $\mathbb{P}(\tilde{Y}_0 = v | \tilde{X}_0 = u) = 1$.*

In optimal transport theory, deterministic couplings are associated with the so-called Monge problem, see Villani (2008) for more context and discussion. A deterministic coupling (\tilde{X}, \tilde{Y}) from X to Y is associated with a map $f : U \rightarrow V$, where $f(u)$ is the (necessarily unique) element $v \in V$ for which $\mathbb{P}(\tilde{Y}_0 = v | \tilde{X}_0 = u) = 1$. In particular, $(\tilde{X}, \tilde{Y}) \stackrel{d}{=} (X, f(X))$. Moreover, as G_2 is strongly connected, $\mathbb{P}(Y_0 = v) > 0$ for each $v \in V$, and the edge-alignment property (Proposition 2) ensures that f is a surjective graph homomorphism from G_1 to G_2 .

Theorem 16. *Suppose G_1 and G_2 are strongly connected, weighted directed networks with associated random walks X and Y , respectively.*

1. *If G_2 is a factor of G_1 with factor map f , then $Y \stackrel{d}{=} f(X)$, and $(X, f(X))$ is a deterministic transition coupling from X to Y .*
2. *If (\tilde{X}, \tilde{Y}) is a deterministic transition coupling from X to Y , then the induced map $f : U \rightarrow V$ is a factor map from G_1 to G_2 .*

When G_2 is a factor of G_1 under f , Theorem 16 ensures that $(X, f(X))$ is a transition coupling of their random walks. If the cost function c is such that $c(u, v)$ is minimized by $v = f(u)$ then, as the next result shows, this coupling is also optimal, and there is a deterministic solution to the NetOTC problem.

Definition 17. *Let f be a factor map from G_1 to G_2 . A cost function c is compatible with f if $c(u, f(u)) \leq c(u, v)$ for each $u \in U$ and $v \in V$.*

One may verify that the cost compatibility condition is satisfied in Example 13 under an Euclidean metric cost.

Corollary 18. *Suppose G_1 and G_2 are strongly connected, weighted directed networks and f is a factor map from G_1 to G_2 . If c is compatible with f then $(X, f(X))$ is an OTC of X and Y .*

An example illustrating Corollary 18 is given in Figure 2. Corollary 18 provides some insight into the structure of the NetOTC problem. If G_1 and G_2 are related by a factor map $f : U \rightarrow V$, then G_2 is essentially a compressed version of the network G_1 . Corollary 18 ensures that an optimal coupling of the random walks on G_1 and G_2 is obtained by running the random walk on G_1 and mapping every state $u \in U$ in this chain to the corresponding

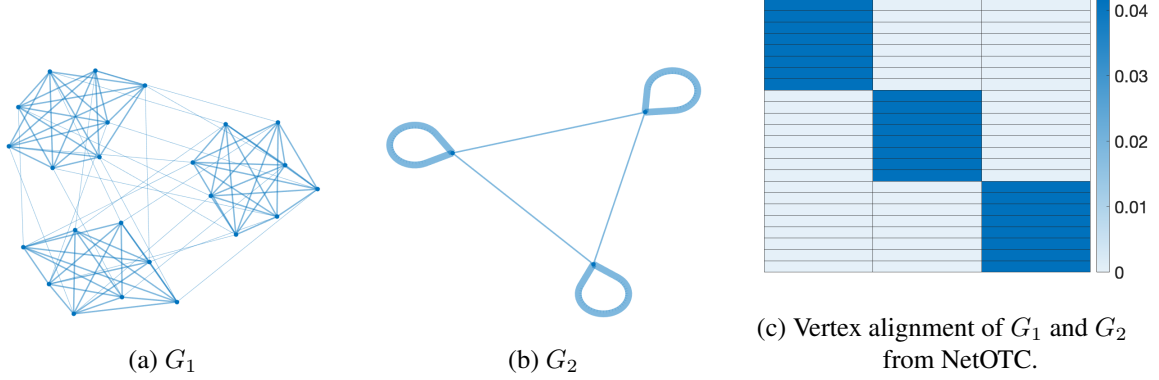


Figure 2: An illustration of the relationship between factors and the NetOTC problem. Under the conditions described in Corollary 18, the NetOTC problem aligns vertices according to the factor map relating the two networks. In this example, G_2 is a factor of G_1 . Figure 2c illustrates the NetOTC vertex alignment, which is supported on pairs of the form $(u, f(u))$.

state $f(u) \in V$. In practice, the conclusion of Corollary 18 approximately holds when the factor condition (9) approximately holds; the results of experiments involving exact and approximate factors are given in Section 6.5. In such situations, NetOTC can be used to identify (approximate) factor maps between G_1 and G_2 .

Under the conditions of Corollary 18, the NetOTC cost and associated vertex and edge alignments will have a special form. In particular, the NetOTC cost will satisfy $\rho(G_1, G_2) = \sum_{u \in U} c(u, f(u))p(u)$ where p is the stationary distribution of the random walk on G_1 . Furthermore, $\pi_v(u, v) = \mathbb{I}(f(u) = v)$ and $\pi_e((u, u'), (v, v')) = \mathbb{I}((f(u), f(u')) = (v, v'))$. Note that, while the deterministic coupling appears as a solution of the NetOTC problem, the NetOTC algorithm itself makes no reference to, and does not require prior information about, the factor map f . The next result provides further information about how NetOTC behaves in the presence of factor maps.

Theorem 19. *Let $G_1, G_2, H_1,$ and H_2 be networks with vertex sets $U, V, A,$ and $B,$ and associated Markov chains $X, Y, W,$ and $Z,$ respectively. Suppose that $f : U \rightarrow A$ and $g : V \rightarrow B$ are factor maps from G_1 to H_1 and G_2 to $H_2,$ and that there are cost functions $c_{ext} : U \times V \rightarrow \mathbb{R}_+$ and $c : A \times B \rightarrow \mathbb{R}_+$ such that $c_{ext}(u, v) = c(f(u), g(v))$.*

1. *If (\tilde{X}, \tilde{Y}) is an optimal transition coupling of X and Y with respect to $c_{ext},$ then $(f(\tilde{X}), g(\tilde{Y}))$ is an optimal transition coupling of W and Z with respect to c .*
2. *If (\tilde{W}, \tilde{Z}) is an optimal transition coupling of W and Z with respect to $c,$ then there exists an optimal transition coupling (\tilde{X}, \tilde{Y}) of X and Y with respect to c_{ext} such that $(f(\tilde{X}), g(\tilde{Y})) \stackrel{d}{=} (\tilde{W}, \tilde{Z}).$*

A simple illustration of Theorem 19 is given in Figure 3. For compatible cost functions, the theorem ensures that an optimal transport plan for the extensions G_1 and G_2 can be transferred through the maps f and g to an optimal transport plan for the factors H_1 and H_2 ; moreover, every optimal transport plan for the factors can be obtained in this way. Thus NetOTC respects factor structure whenever factor structure is present: the NetOTC alignment of the extensions is consistent with the NetOTC alignment of the factors. This is a fundamental property of the NetOTC procedure, in the sense that the operation of NetOTC on the extensions G_1 and G_2 makes no reference to, and requires no knowledge of, the factor maps f and g or the factors H_1 and H_2 . From a practical point of view, if one has access to factor graphs H_1 and $H_2,$ then one could save computational expense by aligning the smaller factor graphs, and Theorem 19 guarantees that the result would be consistent with the alignment of the larger graphs G_1 and G_2 .

6 Example and Experiments

In this section, we illustrate the properties of NetOTC through an example and several numerical experiments. The latter include network classification, network isomorphism, alignment of stochastic block models, and network factors. Complete experimental details may be found in Appendix A. In the example and experiments, we

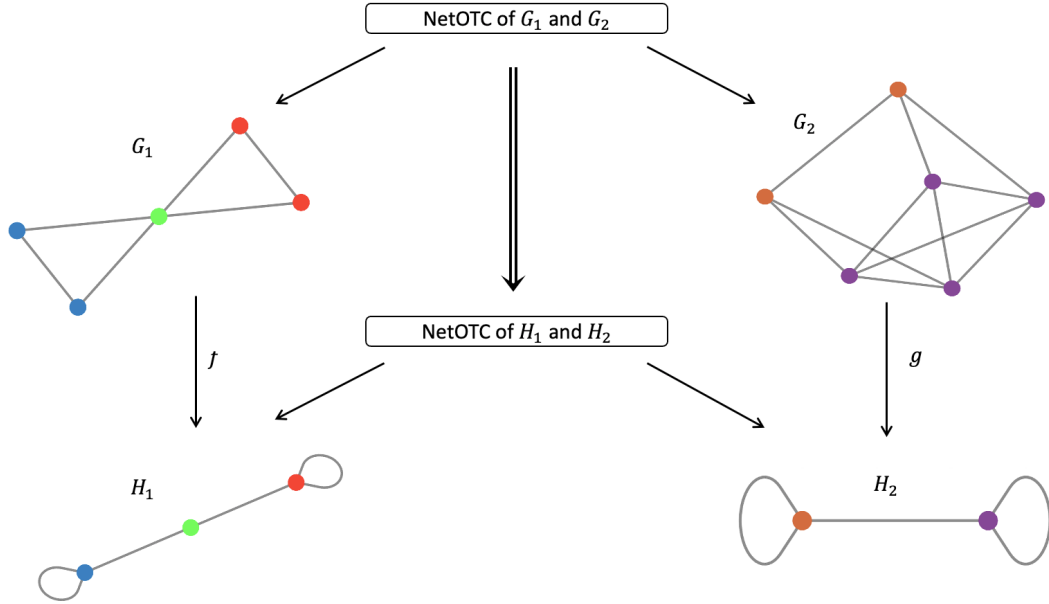


Figure 3: An illustration of Theorem 19. If G_1 and H_1 , and G_2 and H_2 are related by factor maps f and g , respectively, the NetOTC of H_1 and H_2 can be naturally induced by the NetOTC of G_1 and G_2 using the maps f and g .

compare NetOTC to several existing, optimal transport-based approaches to network alignment: marginal optimal transport (OT), Gromov-Wasserstein (GW) (Peyré *et al.*, 2016), Fused Gromov-Wasserstein (FGW) (Titouan *et al.*, 2019; Vayer *et al.*, 2020), and Coordinated Optimal Transport (COPT) (Dong and Sawin, 2020). Here marginal optimal transport refers to the optimal coupling of the stationary distributions of the random walks on the given networks. When applying the FGW method, following Titouan *et al.* (2019); Vayer *et al.* (2020), we use a uniform distribution on the vertices of each network. Code for reproducing the example and experiments may be found at <https://github.com/austinyi/NetOTC>.

6.1 Edge Awareness Example

We begin with a toy example to demonstrate the edge preservation property of NetOTC (see Proposition 2): network G_1 is an octagon network, network G_2 is a copy of G_1 with one edge on the right removed, and network G_3 is topologically identical to G_2 , but its vertices are located in the left half plane. See Figure 4 below.

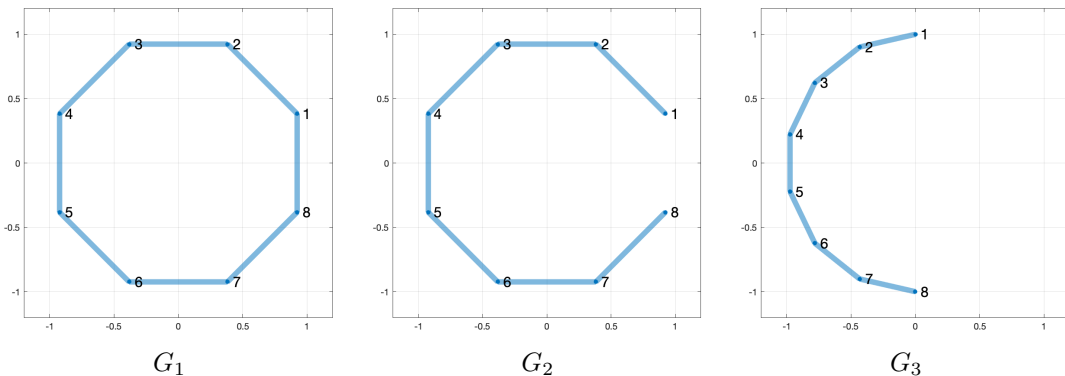


Figure 4: Three networks in which all vertices are located on the unit circle in \mathbb{R}^2 . G_1 is an octagon network. G_2 is obtained by removing an edge G_1 . In G_3 , the vertices are uniformly distributed in the left semicircle.

Table 1 shows the ratio of the costs obtained when comparing different pairs of networks under a cost function

equal to the squared Euclidean distance between vertex positions. We considered the methods NetOTC, OT, and FGW, as they allow the use of the Euclidean cost function. The ratio of the cost between G_2 and G_1 and the cost between G_2 and G_3 varies greatly between the methods. Observe that NetOTC is the only method with a ratio that exceeds 1, that is, NetOTC finds G_2 to be closer to G_3 than G_1 . This example illustrates that NetOTC is sensitive to topological differences between the given networks, and in particular that topological similarity can dominate differences in the vertex costs.

Algorithm	G_2 vs. G_1	G_2 vs. G_3	Ratio
NetOTC	0.5714	0.4464	1.28
OT	0.2857	0.4464	0.64
FGW	0.0313	0.2725	0.11

Table 1: Comparison of OT-based costs between networks in Figure 4.

6.2 Network Classification

In our next experiment, we examine the utility of NetOTC for network classification tasks. We consider a selection of benchmark network datasets from Kersting *et al.* (2016). Each dataset contains a collection of networks with discrete vertex attributes and class labels. We considered the datasets AIDS (Riesen and Bunke, 2008), BZR (Sutherland *et al.*, 2003), Cuneiform (Kriege *et al.*, 2018), MCF-7 (Yan *et al.*, 2008), MOLT-4 (Yan *et al.*, 2008), MUTAG (Debnath *et al.*, 1991), and Yeast (Yan *et al.*, 2008). For each dataset, we employed an attribute-based cost function, where $c(u, v) = 0$ if vertices u and v have the same attribute and $c(u, v) = 1$ otherwise. For each OT-based comparison method, we constructed a 5-nearest neighbor classifier using a random training set containing 80% of the available networks and used this classifier to predict the labels of the remaining networks.

Table 2 shows the average classification accuracy over 5 random samplings of the training and test sets for each comparison method. As the table demonstrates, NetOTC is competitive with other network OT based methods on the classification tasks, outperforming other methods in several cases, without the need for tuning or specification of free parameters.

Algorithm	AIDS	BZR	Cuneiform	MCF-7	MOLT-4	MUTAG	Yeast
NetOTC	88.0 ± 4.9	84.8 ± 6.6	73.2 ± 7.8	92.8 ± 4.2	92.0 ± 2.0	85.4 ± 7.1	90.8 ± 6.4
OT	84.4 ± 6.1	76.4 ± 4.6	71.3 ± 7.7	93.6 ± 3.3	92.0 ± 2.0	63.2 ± 7.3	91.2 ± 7.0
GW	98.8 ± 1.8	78.0 ± 8.5	12.8 ± 4.6	93.6 ± 3.3	91.6 ± 2.6	81.6 ± 7.0	91.6 ± 6.2
FGW	99.2 ± 1.1	80.0 ± 7.1	74.8 ± 3.6	92.8 ± 4.2	91.6 ± 2.6	84.3 ± 8.6	89.2 ± 6.6
COPT	98.0 ± 1.4	73.6 ± 7.9	16.6 ± 3.1	92.4 ± 4.8	91.6 ± 2.6	80.0 ± 5.6	90.4 ± 6.7

Table 2: 5-nearest neighbor classification accuracies for networks with discrete vertex attributes. Average accuracies observed over 5 random samplings of the training and test sets are reported along with their standard deviation.

6.3 Network Isomorphism

Two undirected, unweighted networks $G_1 = (U, E_1)$ and $G_2 = (V, E_2)$ are isomorphic if there is a bijection $\phi : U \rightarrow V$ of their vertex sets that preserves edges in the sense that $(u, u') \in E_1$ if and only if $(\phi(u), \phi(u')) \in E_2$. Determining when two networks are isomorphic, and if so identifying an isomorphism, are important problems in network theory that have received much attention in the literature (McKay and Piperno, 2014; Cordella *et al.*, 2004). In general, it is challenging to find isomorphisms in an efficient fashion (Babai, 2015).

To evaluate the ability of the alignment methods under study to successfully identify network isomorphisms, we carried out the following experiment. Given a network G_1 , we create an isomorphic copy G_2 by applying a permutation ϕ to its vertices. We then applied NetOTC, FGW, GW, and OT to G_1 and G_2 with a degree-based cost function. From each method we obtained a soft vertex alignment $\pi_v : U \times V \rightarrow \mathbb{R}_+$ of the given networks, and from π_v we derived a hard vertex alignment $\psi(u) = \operatorname{argmax}_{v \in V} \pi_v(u, v)$. If the hard alignment ψ is identical to the isomorphism ϕ , the algorithm has successfully identified the isomorphism map. See Appendix A.2 for more details. Figure 5 shows an example of isomorphic “lollipop” networks (another example is shown in Appendix A.2 Figure 8). NetOTC correctly finds the isomorphism map between two isomorphic networks, but the other methods

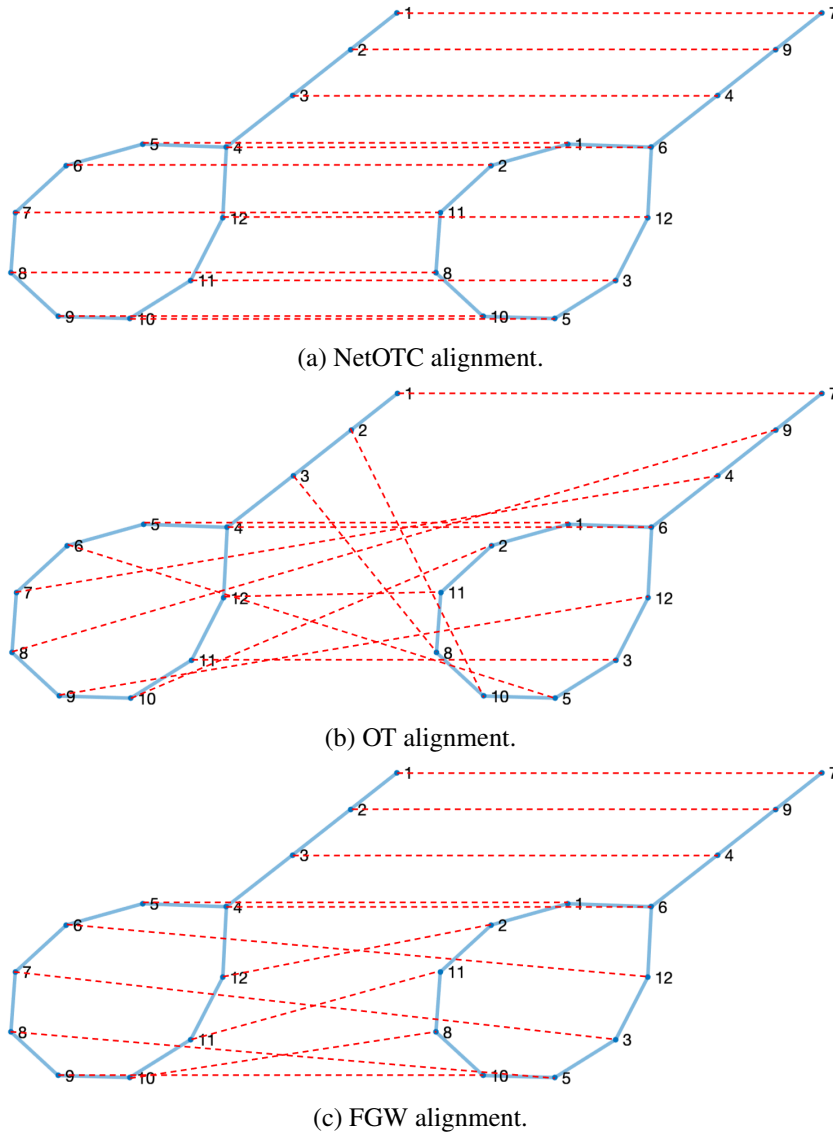


Figure 5: Vertex alignment of two isomorphic lollipop networks obtained by NetOTC, OT, and FGW. NetOTC correctly finds the isomorphism map, while other methods do not.

do not. Note that the cost function used by each method to align the vertices depends only on their degree, and that the majority of the vertices in the lollipop network have degree 2. This example demonstrates that, while the objective function of the NetOTC problem is univariate (it depends only on the cost between vertices at time zero), both the NetOTC distance and optimal transition coupling depend critically on the topological properties of the given networks.

Further experiments demonstrate the ability of NetOTC to recover isomorphisms in different classes of networks: random (Erdos-Renyi) networks, stochastic block models (SBMs), networks with a random weighted $(0,1,2)$ adjacency matrix, and random lollipop networks. Table 3 shows the average performance of each method for 300 random networks of each class. See Appendix A.2 for further details of the network generation process. NetOTC exhibits perfect performance for networks with random adjacency matrices and all types of SBMs, with very high accuracy in Erdos-Renyi and random lollipop networks. On all classes but the random adjacency matrix, the competing methods perform markedly worse. The poor performance of OT demonstrates the substantial performance gains obtained from coupling the full random walks on G_1 and G_2 , rather than their stationary distributions.

	NetOTC	FGW	GW	OT
Erdos-Renyi ($n \in \{6, \dots, 15\}, p = 1/3$)	96.73	71.50	54.67	2.80
Erdos-Renyi ($n \in \{6, \dots, 15\}, p = 2/3$)	94.86	57.19	48.63	8.56
Erdos-Renyi ($n \in \{16, \dots, 25\}, p = 1/4$)	99.64	88.45	69.68	0.00
Erdos-Renyi ($n \in \{16, \dots, 25\}, p = 3/4$)	100.00	71.33	50.00	0.00
SBM (7, 7, 7, 7)	100.00	84.62	54.85	0.00
SBM (10, 8, 6)	100.00	78.33	58.67	0.00
SBM (7, 7, 7)	100.00	71.28	41.89	0.00
Random weighted adjacency matrix $\{0, 1, 2\}$	100.00	96.67	96.33	5.67
Random Lollipop network	98.00	13.67	6.00	0.00

Table 3: Isomorphism map identification success rate (%). We generate 300 random networks in each class. For each random network, we permute its vertices and apply the algorithms to the two isomorphic networks. We report the percentage of times the output alignment of an algorithm yields an isomorphism of the given graphs.

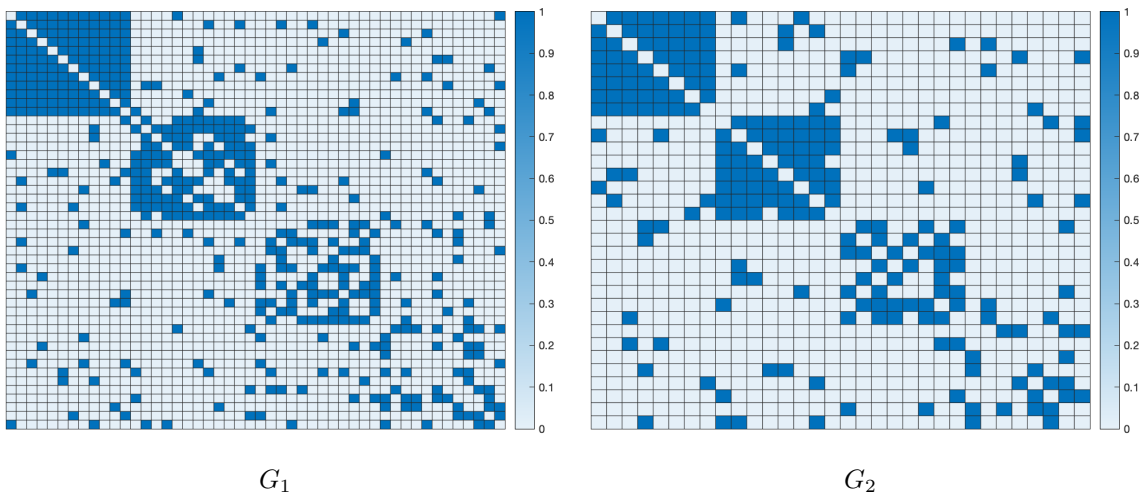


Figure 6: The adjacency matrices of random networks G_1 and G_2 drawn from SBMs. Block structure arises from different connection probabilities within the blocks. Networks G_1 and G_2 are designed to have the same block structure with a different number of vertices.

6.4 Block Alignment in Stochastic Block Models

Stochastic block models (Holland *et al.*, 1983) (SBMs) are frequently used to model random networks with community structure. SBMs have found application in a variety of network problems, including community detection and network clustering, see for example Abbe (2018); Lee and Wilkinson (2019); Abbe and Sandon (2015). In an SBM, each vertex is assigned (deterministically or at random) to one of a small number of groups, also known as blocks. Once group assignment is complete, edges are placed between pairs of vertices independently, with the probability of an edge being present depending on the group assignments of its endpoints. In most cases, edge probabilities are higher within groups than between groups, so that the vertices in a group constitute, informally at least, a community.

We wished to assess the ability of OT-based comparison methods to align the vertices and edges of stochastically equivalent blocks in SBMs of different sizes. To this end, we generated 10 realizations G_1, G_2 of SBMs with 4 blocks. In each case, the network G_1 had 12 vertices per block, and G_2 had 8 vertices per block. For each network, the within block connection probabilities were 1, 0.8, 0.6, and 0.4, while the between block connection probability was equal to 0.1. The adjacency matrix of a typical realization of G_1 and G_2 is depicted in Figure 6. Note that the networks G_1 and G_2 are undirected and unweighted.

We applied the five comparison methods under study to each of the 10 realizations of G_1 and G_2 using the standardized degree-based cost function. Each method returns a vertex alignment $\pi_v : U \times V \rightarrow \mathbb{R}_+$ associated with the respective optimal transport plans. Vertex alignment accuracy was assessed by summing π_v over vertex pairs in corresponding blocks, i.e., blocks with the same connection probability.

As described above, the NetOTC optimal transport plan also provides a native edge alignment $\pi_e : U^2 \times V^2 \rightarrow \mathbb{R}_+$. For other methods, we formed an edge alignment by setting $\pi_e((u, u'), (v, v')) = \pi_v(u, v)\pi_v(u', v')$. Edge alignment accuracy was evaluated by summing the alignment probabilities of all pairs of edges connecting stochastically equivalent blocks, i.e., summing all $\pi_e((u, u'), (v, v'))$ where u and v , and u' and v' are from blocks with equal connection probabilities.

Figure 7 shows the vertex and edge alignment accuracies for each of the methods tested. As background, we note that random guessing yields an accuracy of 25% for vertex alignment and 6.25% for edge alignment. For vertex alignment, NetOTC, GW, and FGW exhibit similar performance (substantially better than random guessing) while OT and COPT do worse. As indicated by the error bars in Figure 7, the vertex alignment accuracy of NetOTC has a lower variance than the accuracies of OT, GW, and FGW. As expected, NetOTC outperforms other methods from the standpoint of edge alignment.

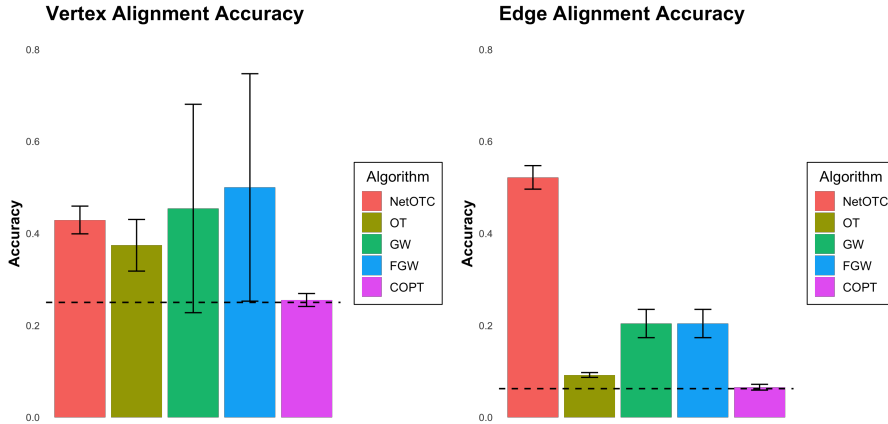


Figure 7: SBM alignment accuracies. Average accuracies observed over 10 random pairs of SBMs are reported along with their standard deviation. The horizontal dashed line in each plot indicates the accuracy of random guessing.

6.5 Network Factors

Lastly, we considered the task of aligning corresponding vertices when the network G_2 is a factor of G_1 and the cost is compatible with the factor map (see Section 5.4). We construct networks G_1 and G_2 via vertex embeddings in \mathbb{R}^5 as follows. The network G_2 has 6 vertices, each associated with a feature vector generated from a 5-dimensional normal distribution with mean zero and variance $\sigma^2 \mathbf{I}$. The network G_1 has 30 vertices, each associated with a feature vector sampled from a 6-component Gaussian mixture model. The means of the 6 components correspond to the feature vectors associated with the 6 vertices of G_2 , while the variances are \mathbf{I}_5 . Here, the factor map f is determined by the component from which the feature vector was sampled. Next, we randomly set the edge weights of network G_2 to an integer between 1 and 10. Then, the edge weights of network G_1 are randomly determined so that equation (9) holds, and therefore G_2 is a factor of G_1 . The networks considered are undirected, in order to enable comparison with other methods. See Table 5 of Appendix A.4 for results on directed networks; there was no significant difference in the performance of NetOTC between directed and undirected networks. The experiment was repeated in a setting where G_2 is an approximate factor of G_1 , that is, when the factor condition only holds approximately. See Appendix A.4 for explanations of how we generated an approximate factor.

NetOTC, FGW, and OT were applied to the generated networks G_1 and G_2 using an embedding-based cost equal to the squared Euclidean distances between the vectors associated with the vertices. Table 4 reports the vertex alignment accuracy of each method for different values of the variance σ^2 . Vertex alignment accuracy was assessed by summing the mass of the optimal coupling on factor pairs of the form $(u, f(u))$. NetOTC outperforms the other methods, with the performance gap growing as σ decreases. For an exact factor with compatible cost, which occurs when $\sigma = 2.5$, NetOTC returns a perfect alignment, as guaranteed by Corollary 18. Results from other cases demonstrate that the performance of NetOTC is robust when the factor and cost conditions hold only approximately. It is also noteworthy that FGW and OT yield nearly identical alignment accuracy in all cases.

	Exact factor			Approximate factor		
	NetOTC	FGW	OT	NetOTC	FGW	OT
$\sigma = 2.5$	100.00 \pm 0.00	98.17 \pm 3.95	98.38 \pm 3.40	98.57 \pm 0.20	98.07 \pm 4.55	98.32 \pm 3.96
$\sigma = 2.0$	99.95 \pm 0.46	96.57 \pm 5.22	96.75 \pm 5.08	98.09 \pm 1.64	95.83 \pm 5.35	96.00 \pm 5.11
$\sigma = 1.5$	97.45 \pm 5.10	90.20 \pm 8.24	90.57 \pm 8.18	96.43 \pm 4.40	91.23 \pm 7.85	91.65 \pm 7.72
$\sigma = 1.0$	81.60 \pm 13.88	73.23 \pm 12.08	73.85 \pm 12.05	79.44 \pm 12.14	72.00 \pm 11.74	72.00 \pm 12.06

Table 4: Undirected networks: alignment accuracies of network factors. Average accuracies observed over 100 random network factors are reported along with their standard deviation.

7 Conclusion

In this paper we have introduced the NetOTC method for comparison and alignment of weighted networks. This new approach is based on constrained optimal transport of the random walks (Markov chains) associated with each network. Given two networks and a vertex-related cost function, NetOTC identifies an optimal coupling between their associated random walks that minimizes the expected cost at time zero. NetOTC applies to both directed and undirected networks, as well as networks with different numbers of nodes. Once edge weights and node-cost functions are specified, NetOTC has no free parameters and involves no randomization. The expected cost resulting from the optimal coupling serves as a numerical measure of the dissimilarity between the networks. In addition, the optimal transport plan itself offers interpretable, probabilistic alignments of both vertices and edges between the two networks.

We have demonstrated that NetOTC effectively incorporates global and local structure by focusing on coupling the full random walks, rather than stationary or other node-level distributions. We established several theoretical properties of NetOTC that support its use, including metric properties of the minimizing cost as well as its connection with short- and long-run average cost. A key feature of NetOTC is that it respects edges: edges are aligned with positive probability only if they are present in the given networks. In addition, we introduced a new notion of factor for weighted networks and established a close connection between factors and NetOTC. Complementing the theory, we presented simulations and numerical experiments showing that NetOTC is competitive with, and sometimes superior to, other optimal transport-based network comparison methods in the literature. In particular, NetOTC showed promise in identifying isomorphic networks using a local (degree-based) cost function.

8 Proofs

In this section, we provide the proof of our results. Before proceeding, we introduce some necessary background. Given two stationary processes $X = X_0, X_1, \dots$ and $Y = Y_0, Y_1, \dots$ taking values in finite sets U and V , respectively, and a cost $c : U \times V \rightarrow \mathbb{R}_+$, the optimal joining distance $\mathcal{S}_c(X, Y)$ is the minimum of $\mathbb{E}[c(\tilde{X}_0, \tilde{Y}_0)]$ over stationary couplings (\tilde{X}, \tilde{Y}) of X and Y . Stationary couplings are referred to as *joinings* in the ergodic theory literature (Furstenberg, 1967; de la Rue, 2009). As every transition coupling of stationary Markov chains X and Y is also a joining, we have

$$\mathcal{S}_c(X, Y) \leq \min_{(\tilde{X}, \tilde{Y}) \in \Pi_{TC}(X, Y)} \mathbb{E}c(\tilde{X}_0, \tilde{Y}_0) = \rho(G_1, G_2) \quad (12)$$

When c is a metric, $\mathcal{S}_c(\cdot, \cdot)$ is a metric between stationary processes (Gray *et al.*, 1975).

Now we introduce some additional notation. For any finite set S , let Δ_S denote the set of probability distributions on S . We will regard $\lambda \in \Delta_S$ as a row vector, and write $\lambda(s)$ for the λ -probability of $s \in S$. If $g : S \rightarrow \mathbb{R}$ is any function, let $\langle \lambda, g \rangle = \sum_{s \in S} \lambda(s)g(s)$, which is the expectation of g with respect to λ . For stochastic matrices (equivalently, Markov transition kernels) P and Q let $\Pi_{TC}(P, Q)$ denote the set of stochastic matrices R satisfying the transition coupling condition (1). By Proposition 4 in O’Connor *et al.* (2022) the NetOTC cost can be written as $\rho(G_1, G_2) = \min \{ \langle \lambda, c \rangle : R \in \Pi_{TC}(P, Q), \lambda R = \lambda, \lambda \in \Delta_{U \times V} \}$.

8.1 Result for NetOTC Edge Preservation

Proposition 2. *Let π_e be the NetOTC edge alignment of networks $G_1 = (U, E_1, w_1)$ and $G_2 = (V, E_2, w_2)$ based on the optimal transport plan (X^*, Y^*) . If $\pi_e((u, u'), (v, v')) > 0$ then $(u, u') \in E_1$ and $(v, v') \in E_2$.*

Proof. Let P and Q be the transition kernels associated with graphs G_1 and G_2 , and let

$$\lambda^*, \mathbf{R}^* = \operatorname{argmin}_{\lambda, \mathbf{R}} \{ \langle \lambda, c \rangle : \mathbf{R} \in \Pi_{\text{TC}}(P, Q), \lambda \mathbf{R} = \lambda, \lambda \in \Delta_{U \times V} \},$$

be a solution for the NetOTC problem. The edge alignment probability can be expressed in terms of λ^*, \mathbf{R}^* as $\pi_e((u, u'), (v, v')) = \lambda^*(u, v) \mathbf{R}^*(u', v' | u, v)$. Since $\mathbf{R}^* \in \Pi_{\text{TC}}(P, Q)$ and $\pi_e((u, u'), (v, v')) > 0$, we have

$$\begin{aligned} P(u' | u) &= \sum_{\tilde{v} \in V} \mathbf{R}^*(u', \tilde{v} | u, v) \geq \mathbf{R}^*(u', v' | u, v) > 0, \\ Q(v' | v) &= \sum_{\tilde{u} \in U} \mathbf{R}^*(\tilde{u}, v' | u, v) \geq \mathbf{R}^*(u', v' | u, v) > 0, \end{aligned}$$

which implies $(u, u') \in E_1$ and $(v, v') \in E_2$. □

8.2 Properties of $\rho(G_1, G_2)$

Proposition 4. *Let G_1 and G_2 be networks with associated random walks X and Y . Then*

$$\rho(G_1, G_2) = \min_{(\tilde{X}, \tilde{Y}) \in \Pi_{\text{TC}}(X, Y)} \mathbb{E} \bar{c}(\tilde{X}, \tilde{Y}),$$

and the optimal transport plans minimizing $\mathbb{E} \bar{c}(\tilde{X}, \tilde{Y})$ coincide with those minimizing $\mathbb{E} c(\tilde{X}_0, \tilde{Y}_0)$.

Proof. Let (\tilde{X}, \tilde{Y}) be a transition coupling of X and Y . As (\tilde{X}, \tilde{Y}) is stationary, the ergodic theorem (Theorem C.1 of Levin and Peres (2017)) ensures that the limit

$$\hat{c}(\tilde{X}, \tilde{Y}) := \lim_k c_k(\tilde{X}_0^{k-1}, \tilde{Y}_0^{k-1})$$

exists almost surely and that $\mathbb{E} \hat{c}(\tilde{X}, \tilde{Y}) = \mathbb{E} c(\tilde{X}, \tilde{Y})$. It then follows from the definition of \bar{c} that

$$\mathbb{E} \bar{c}(\tilde{X}, \tilde{Y}) = \mathbb{E} \hat{c}(\tilde{X}, \tilde{Y}) = \mathbb{E} c(\tilde{X}, \tilde{Y}).$$

Taking minima over the set of all transition couplings of X and Y yields the result. □

Proposition 5. *Let G_1 and G_2 be networks with associated random walks X and Y . For each $k \geq 1$*

$$\rho(G_1, G_2) \geq \min \mathbb{E} c_k(\tilde{X}_0^{k-1}, \tilde{Y}_0^{k-1}),$$

where the minimum is over the family of all couplings of X_0^{k-1} and Y_0^{k-1} .

Proof. Every transition coupling of X and Y is also a joining of X and Y and therefore, as noted in (12), $\rho(G_1, G_2) \geq \mathcal{S}_c(X, Y)$. Let (\tilde{X}, \tilde{Y}) be any joining of X and Y . Stationarity of (\tilde{X}, \tilde{Y}) implies that

$$\mathbb{E} c(\tilde{X}_0, \tilde{Y}_0) = \mathbb{E} c_k(\tilde{X}_0^{k-1}, \tilde{Y}_0^{k-1})$$

and therefore $\mathcal{S}_c(X, Y) = \mathcal{S}_{c_k}(X, Y)$. Moreover, $(\tilde{X}_0^{k-1}, \tilde{Y}_0^{k-1})$ is also a coupling of X_0^{k-1} and Y_1^k so

$$\mathcal{S}_{c_k}(X, Y) \geq \min_{(\tilde{X}_0^{k-1}, \tilde{Y}_0^{k-1}) \in \Pi(X_0^{k-1}, Y_0^{k-1})} \mathbb{E} c_k(\tilde{X}_0^{k-1}, \tilde{Y}_0^{k-1}).$$

Combining these inequalities gives the result. □

8.3 Results for Undirected Networks with a Common Vertex Set

Here we consider undirected networks on a common vertex set. We assume that the networks are connected. Throughout this section, we will make use of the well-known fact that the stationary distribution of a simple random walk $X = X_0, X_1, \dots$ on a connected undirected network $G = (U, E, w)$ satisfies $p(u) = d(u)/D$, where $d(u)$ is the weighted degree of u and D is the sum of all the weights in the network.

Proposition 7. *Connected undirected networks G_1 and G_2 are equivalent if and only if their respective random walks are identical.*

Proof. Let $d_1(u) = \sum_{u' \in U} w_1(u, u')$ and $d_2(u) = \sum_{u' \in U} w_2(u, u')$ be the degree functions for G_1 and G_2 . Suppose first that $G_1 \sim G_2$ and thus there exists $C > 0$ such that $w_1(u, u') = Cw_2(u, u')$ for every $u, u' \in U$. Then the two transition matrices P and Q associated with G_1 and G_2 are equal since

$$P(u'|u) = \frac{w_1(u, u')}{d_1(u)} = \frac{w_2(u, u')}{d_2(u)} = Q(u'|u).$$

Suppose now that P and Q are equal. Then for every $(u, u') \in E_1$, we have

$$\frac{w_1(u, u')}{d_1(u)} = \frac{w_2(u, u')}{d_2(u)},$$

or equivalently $w_1(u, u') = C_u w_2(u, u')$ where $C_u = d_1(u)/d_2(u)$. As G_1 and G_2 are undirected, it is easy to see that $C_u = C_{u'}$. As G_1 and G_2 are connected, there exists a sequence of edges $(u_1, u_2), (u_2, u_3), \dots, (u_{n-1}, u_n) \in E$ such that $U \subseteq \{u_1, \dots, u_n\}$. Repeating the arguments above for all edges in this sequence we conclude that $C_u = C_{u'}$ for every $u, u' \in U$, and it follows that $G_1 \sim G_2$. \square

Proposition 8. *If the cost function $c : U \times U \rightarrow \mathbb{R}_+$ satisfies the properties of a metric on U , then ρ is a metric on the equivalence classes of undirected networks with vertex set contained in U defined by \sim .*

Proof. The symmetry of ρ is clear. It is established in Proposition 25 of O'Connor *et al.* (2022) that the optimal transition coupling cost satisfies the triangle inequality for Markov chains when the cost c does, and therefore ρ satisfies the triangle inequality. Thus it suffices to show that $\rho(G_1, G_2) = 0$ if and only if $G_1 \sim G_2$. Let G_1 and G_2 be networks satisfying $G_1 \sim G_2$ with associated transition matrices P and Q . By Proposition 7, P and Q are equal and clearly $\rho(G_1, G_2) = 0$ since $\langle \lambda, c \rangle = 0$ is achieved by λ satisfying $\lambda(u, v) = p(u)\mathbb{I}(u = v)$, which is stationary for the transition coupling satisfying

$$R(u', v'|u, v) = \begin{cases} P(u'|u)\mathbb{I}(u' = v') & u = v \\ P(u'|u)P(v'|v) & \text{otherwise} \end{cases}.$$

Now suppose that $G_1 \not\sim G_2$. By Proposition 7, P and Q are necessarily distinct, and consequently so are their associated stationary Markov chains. As it defines a distance on stationary processes $\mathcal{S}_c(X, Y) > 0$, and applying (12), we conclude that $\rho(G_1, G_2) > 0$ as well. \square

Proposition 10. *Let G_1 and G_2 be undirected networks with the same vertex set. Let $d_1(u)$ and $d_2(u)$ be the degree functions of G_1 and G_2 , respectively, and assume that each network has a total degree of D . Then under the zero-one cost $c(u, u') = \mathbb{I}(u \neq u')$,*

- $\rho(G_1, G_2) \geq \frac{1}{2D} \sum_{u \in U} |d_1(u) - d_2(u)|$
- $\rho(G_1, G_2) \geq \frac{1}{4D} \sum_{u, u' \in U} |w_1(u, u') - w_2(u, u')|$

Proof. The random walks X and Y associated with G_1 and G_2 have stationary distributions $p(u) = d_1(u)/D$ and $q(u) = d_2(u)/D$. Using the well-known connection between total variation distance and optimal transport under the 0-1 cost (see, e.g., Equation 6.11 of Villani (2008)), we have

$$\begin{aligned} \min_{(\tilde{X}_0, \tilde{Y}_0) \in \Pi(X_0, Y_0)} \mathbb{E}c(\tilde{X}_0, \tilde{Y}_0) &= \min_{(\tilde{X}_0, \tilde{Y}_0) \in \Pi(X_0, Y_0)} \mathbb{E}\mathbb{I}(\tilde{X}_0 \neq \tilde{Y}_0) \\ &= \frac{1}{2} \sum_{u \in U} |p(u) - q(u)| = \frac{1}{2D} \sum_{u \in U} |d_1(u) - d_2(u)|. \end{aligned}$$

Applying Proposition 5 yields the bound for $k = 1$. To obtain the bound for $k = 2$, let $\delta_2((u, u'), (v, v')) = \mathbb{I}((u, u') \neq (v, v'))$ and note that

$$\delta_2((u, u'), (v, v')) \leq \mathbb{I}(u \neq v) + \mathbb{I}(u' \neq v') = 2c_2((u, v), (u', v')).$$

By Proposition 5,

$$\rho(G_1, G_2) \geq \min_{(\tilde{X}_0^1, \tilde{Y}_0^1) \in \Pi(X_0^1, Y_0^1)} \mathbb{E}c_2(\tilde{X}_0^1, \tilde{Y}_0^1) \geq \frac{1}{2} \min_{(\tilde{X}_0^1, \tilde{Y}_0^1) \in \Pi(X_0^1, Y_0^1)} \mathbb{E}\delta_2(\tilde{X}_0^1, \tilde{Y}_0^1).$$

Then using the connection between the transport cost with respect to δ_2 and the total variation distance once again, we obtain

$$\begin{aligned}
\rho(G_1, G_2) &\geq \frac{1}{4} \sum_{u, u' \in U} |\mathbb{P}(X_0^1 = (u, u')) - \mathbb{P}(Y_0^1 = (u, u'))| \\
&= \frac{1}{4} \sum_{u, u' \in U} |p(u)\mathbb{P}(X_1 = u' | X_0 = u) - q(u)\mathbb{P}(Y_1 = u' | Y_0 = u)| \\
&= \frac{1}{4} \sum_{u, u' \in U} \left| \frac{d_1(u)}{D} \frac{w_1(u, u')}{d_1(u)} - \frac{d_2(u)}{D} \frac{w_2(u, u')}{d_2(u)} \right| \\
&= \frac{1}{4D} \sum_{u, u' \in U} |w_1(u, u') - w_2(u, u')|.
\end{aligned}$$

□

8.4 Results Concerning Network Factors

In this section, we prove the results about factor maps, including Theorems 16 and 19.

Proposition 14. *If (\tilde{X}, \tilde{Y}) is a stationary Markov coupling corresponding to a strongly connected network H with vertex set W , then (\tilde{X}, \tilde{Y}) is a transition coupling of X and Y if and only if the restriction of π_U to W is a factor map from H to G_1 and the restriction of π_V to W is a factor map from H to G_2 .*

Proof. In this setting, the conditions in Definition 1 for (\tilde{X}, \tilde{Y}) to be a transition coupling are precisely equivalent to Condition 9 for the restrictions of π_U and π_V to W . □

Theorem 16. *Suppose G_1 and G_2 are strongly connected, weighted directed networks with associated random walks X and Y , respectively.*

1. *If G_2 is a factor of G_1 with factor map f , then $Y \stackrel{d}{=} f(X)$, and $(X, f(X))$ is a deterministic transition coupling from X to Y .*
2. *If (\tilde{X}, \tilde{Y}) is a deterministic transition coupling from X to Y , then the induced map $f : U \rightarrow V$ is a factor map from G_1 to G_2 .*

Proof. To prove 1., let f be a factor map from G_1 to G_2 . We first show $Y \stackrel{d}{=} f(X)$. In order to simplify notation, we will let $f(X_0^{n-1}) = f(X_0), \dots, f(X_{n-1})$. Let us prove by induction that for any $v_0^n \in V$, we have

$$\mathbb{P}(f(X_0^n) = v_0^n) = \mathbb{P}(Y_0^n = v_0^n).$$

The base case ($n = 0$) is immediate from Equation (11). For the inductive step, we suppose it is true for some $n \geq 0$. Let $v_0^{n+1} \in V$. Then we have

$$\begin{aligned}
\mathbb{P}(f(X_0^n) = v_0^{n+1}) &= \sum_{u_0^{n+1} \in f^{-1}(v_0^{n+1})} \mathbb{P}(X_0^{n+1} = u_0^{n+1}) \\
&= \sum_{u_0^{n+1} \in f^{-1}(v_0^{n+1})} \mathbb{P}(X_0^n = u_0^n) \cdot \mathbb{P}(X_{n+1} = u_{n+1} | X_0^n = u_0^n) \\
&= \sum_{u_0^n \in f^{-1}(v_0^n)} \mathbb{P}(X_0^n = u_0^n) \cdot \sum_{u_{n+1} \in f^{-1}(v_{n+1})} \mathbb{P}(u_{n+1} | u_n) \\
&= \mathbb{Q}(v_{n+1} | v_n) \cdot \sum_{u_0^n \in f^{-1}(v_0^n)} \mathbb{P}(X_0^n = u_0^n) \\
&= \mathbb{P}(Y_{n+1} = v_{n+1} | Y_n = v_n) \cdot \mathbb{P}(Y_0^n = v_0^n) \\
&= \mathbb{P}(Y_0^{n+1} = v_0^{n+1}),
\end{aligned}$$

where we have used Equation (10) and the inductive hypothesis.

Next, we show that $(X, f(X))$ is a transition coupling of X and Y . We begin by verifying that $(X, f(X))$ is Markov. Fixing $(u, v) \in U \times V$ and $n \geq 1$, we have

$$\begin{aligned} \mathbb{P}((X_n, f(X_n)) = (u, v) | \{(X_i, f(X_i))\}_{i < n}) &= \mathbb{P}((X_n, f(X_n)) = (u, v) | \{X_i\}_{i < n}) \\ &= \mathbb{P}(X_n = u | \{X_i\}_{i < n}) \mathbb{I}(f(u) = v) \\ &= \mathbb{P}(X_n = u | X_{n-1}) \mathbb{I}(f(u) = v) \\ &= \mathbb{P}((X_n, f(X_n)) = (u, v) | X_{n-1}) \\ &= \mathbb{P}((X_n, f(X_n)) = (u, v) | (X_{n-1}, f(X_{n-1}))), \end{aligned}$$

so the process $(X, f(X))$ is Markov.

This Markov chain clearly has a U marginal that is equal in distribution to X and the V marginal is equal in distribution to Y as we proved above. Thus the joint process is a coupling of X and Y . So it suffices to check the transition coupling condition. Let $R \in [0, 1]^{|U||V| \times |U||V|}$ denote the transition matrix satisfying

$$R(u', v' | u, v) = \begin{cases} P(u' | u) \mathbb{I}(f(u') = v') & f(u) = v \\ P(u' | u) Q(v' | v) & \text{otherwise} \end{cases}.$$

Let p be the stationary distribution of X . Then $\lambda(u, v) = p(u) \mathbb{I}(f(u) = v)$ is equal in distribution to $(X_0, f(X_0))$. Observe that for all $(u', v') \in U \times V$, we have

$$\begin{aligned} \sum_{(u, v) \in U \times V} \lambda(u, v) R(u', v' | u, v) &= \sum_{(u, v) \in U \times V} p(u) \mathbb{I}(f(u) = v) P(u' | u) \mathbb{I}(f(u') = v') \\ &= \mathbb{I}(f(u') = v') \sum_{v \in V} \sum_{u \in f^{-1}(v)} p(u) P(u' | u) \\ &= \mathbb{I}(f(u') = v') \sum_{u \in U} p(u) P(u' | u) \\ &= p(u') \mathbb{I}(f(u') = v') \\ &= \lambda(u', v'), \end{aligned}$$

and therefore λ is stationary for R . So lastly, we only need to show that $R \in \Pi_{TC}(P, Q)$. For pairs $(u, v) \in U \times V$ with $f(u) \neq v$, we see that $R(\cdot | u, v)$ is the independent coupling of $P(\cdot | u)$ and $Q(\cdot | v)$, which clearly satisfies the transition coupling condition. Thus we need only check the transition coupling condition for pairs (u, v) satisfying $f(u) = v$. Let $u, u' \in U$ and $v \in V$ and suppose that $f(u) = v$. Then

$$\sum_{v' \in V} R(u', v' | u, v) = \sum_{v' \in V} P(u' | u) \mathbb{I}(f(u') = v') = P(u' | u).$$

Now checking the other half of the transition coupling condition, let $u \in U$ and $v, v' \in V$ be such that $f(u) = v$. Then by Equation (10), we have

$$\sum_{u' \in U} R(u', v' | u, v) = \sum_{u' \in U} P(u' | u) \mathbb{I}(f(u') = v') = \sum_{u' \in f^{-1}(v')} P(u' | u) = Q(v' | v).$$

Thus $(X, f(X))$ is a transition coupling of X and Y . It is forward-deterministic by construction.

Now we prove 2. To that end, suppose (\tilde{X}, \tilde{Y}) is a forward-deterministic coupling of X and Y , and let $f : U \rightarrow V$ be the induced map. For notation, let R be the transition matrix associated to the joint Markov chain (\tilde{X}, \tilde{Y}) . To verify that f is a factor map, let $v, v' \in V$ and $u \in f^{-1}(v)$. Since (\tilde{X}, \tilde{Y}) is forward deterministic, for every $u' \in f^{-1}(v')$ we have that $P(u' | u) = R((u', v') | (u, v))$. Then, also using the transition coupling property of R , we see that

$$\sum_{u' \in f^{-1}(v')} P(u' | u) = \sum_{u' \in f^{-1}(v')} R((u', v') | (u, v)) = \sum_{u' \in U} R((u', v') | (u, v)) = Q(v', v).$$

□

Corollary 18. *Suppose G_1 and G_2 are strongly connected, weighted directed networks and f is a factor map from G_1 to G_2 . If c is compatible with f then $(X, f(X))$ is an OTC of X and Y .*

Proof. By part 1. of Theorem 16, we have that $(X, f(X))$ is a transition coupling of X and Y . Let (\tilde{X}, \tilde{Y}) be any transition coupling of X and Y . Then,

$$\mathbb{E}c(\tilde{X}_0, \tilde{Y}_0) \geq \mathbb{E}c(\tilde{X}_0, f(\tilde{X}_0)) = \mathbb{E}c(X_0, f(X_0)).$$

Taking an infimum over all transition couplings (\tilde{X}, \tilde{Y}) of X and Y , we conclude that $(X, f(X))$ is an optimal transition coupling of X and Y , as desired. \square

In the following proof of our two-factor result (Theorem 19), we will use the notion of relatively independent couplings. Suppose X, Y , and Z are random variables and there are maps f and g such that $f(X) \stackrel{d}{=} Z$ and $g(Y) \stackrel{d}{=} Z$. The main property that we need is that there exists a coupling (\tilde{X}, \tilde{Y}) of X and Y such that $f(\tilde{X}) = g(\tilde{Y})$ almost surely. The existence of such a coupling is usually demonstrated by constructing the *relatively independent coupling* of X and Y over Z , which is defined by the property that

$$\mathbb{P}(\tilde{X} \in A, \tilde{Y} \in B) = \mathbb{E}[\mathbb{P}(X \in A \mid Z) \cdot \mathbb{P}(Y \in B \mid Z)],$$

where the expectation is taken with respect to Z . In words, the relatively independent coupling makes \tilde{X} and \tilde{Y} conditionally independent given Z . This construction is useful in optimal transport for proving the triangle inequality. In the context of ergodic theory, when the random variables are replaced by stationary processes, it is called the relatively independent joining of X and Y (De La Rue, 2005). We note if the stationary processes are the random walks on some strongly connected networks and the maps f and g are factor maps in the sense of Section 5.4, then the relatively independent joinings are in fact transition couplings.

Proposition 20. *Suppose $G_1 = (U, E_1, w_1)$, $G_2 = (V, E_2, w_2)$, and $G_3 = (W, E_3, w_3)$ are strongly connected weighted directed networks with associated random walks X, Y , and Z . Further suppose that there are factor maps $f : U \rightarrow W$ from G_1 to G_3 and $g : V \rightarrow W$ from G_2 to G_3 . Then there is a transition coupling (\tilde{X}, \tilde{Y}) of X and Y such that $f(\tilde{X}) = g(\tilde{Y})$ holds almost surely.*

Proof. Define the coupling (\tilde{X}, \tilde{Y}) to be the Markov chain with stationary distribution r and transition kernel R given as follows. For $w \in W$ with $\mathbb{P}(Z_0 = w) > 0$ and $(u, v) \in U \times V$ such that $f(u) = g(v) = w$, let

$$r(u, v) = \frac{\mathbf{p}(u) \cdot \mathbf{q}(v)}{\mathbb{P}(Z_0 = w)},$$

and otherwise let $r(u, v) = 0$. Furthermore, for $(w, w') \in E_3$ and $(u, v), (u', v') \in U \times V$ such that $f(u) = g(v) = w$ and $f(u') = g(v') = w'$, let

$$R((u', v') \mid (u, v)) = \frac{\mathbf{P}(u' \mid u) \cdot \mathbf{Q}(v' \mid v)}{\mathbb{P}(Z_1 = w' \mid Z_0 = w)}.$$

If $f(u) = g(v) = w$ while (u', v') does not satisfy $f(u') = g(v') = w'$, then let $R((u', v') \mid (u, v)) = 0$. Finally, if $f(u) = g(v) = w$ does not hold, then let $R((u', v') \mid (u, v)) = \mathbf{P}(u' \mid u) \cdot \mathbf{Q}(v' \mid v)$. Using this definition, one may immediately verify Condition (1), and thus (\tilde{X}, \tilde{Y}) is a transition coupling of X and Y . Furthermore, by construction we have $f(\tilde{X}) = g(\tilde{Y})$ almost surely. \square

With this result in hand, we may now proceed to our second main result concerning factors.

Theorem 19. *Let G_1, G_2, H_1 , and H_2 be networks with vertex sets U, V, A , and B , and associated Markov chains X, Y, W , and Z , respectively. Suppose that $f : U \rightarrow A$ and $g : V \rightarrow B$ are factor maps from G_1 to H_1 and G_2 to H_2 , and that there are cost functions $c_{ext} : U \times V \rightarrow \mathbb{R}_+$ and $c : A \times B \rightarrow \mathbb{R}_+$ such that $c_{ext}(u, v) = c(f(u), g(v))$.*

1. *If (\tilde{X}, \tilde{Y}) is an optimal transition coupling of X and Y with respect to c_{ext} , then $(f(\tilde{X}), g(\tilde{Y}))$ is an optimal transition coupling of W and Z with respect to c .*
2. *If (\tilde{W}, \tilde{Z}) is an optimal transition coupling of W and Z with respect to c , then there exists an optimal transition coupling (\tilde{X}, \tilde{Y}) of X and Y with respect to c_{ext} such that $(f(\tilde{X}), g(\tilde{Y})) \stackrel{d}{=} (\tilde{W}, \tilde{Z})$.*

Proof. Let (\tilde{X}, \tilde{Y}) be a transition coupling of X and Y . Since f and g are factor maps, we see that $(f(\tilde{X}), g(\tilde{Y}))$ is a transition coupling of W and Z . Then by the compatibility condition on the cost function we have

$$\mathbb{E}c_{ext}(\tilde{X}, \tilde{Y}) = \mathbb{E}c(f(\tilde{X}), g(\tilde{Y})). \quad (13)$$

To ease the notational burden of the following argument, we do not distinguish between different couplings of the same random variables. In particular, the notation \tilde{X} may represent formally distinct random variables (defined on different probability spaces) from one instance to the next, although it always denotes a random variable that is equal in distribution to X .

Now let (\tilde{W}, \tilde{Z}) be a transition coupling of W and Z . We claim that there exists a transition coupling (\tilde{X}, \tilde{Y}) such that $(f(\tilde{X}), g(\tilde{Y})) \stackrel{d}{=} (\tilde{W}, \tilde{Z})$. To exhibit the desired transition coupling, we repeatedly use Proposition 20. Let $(\tilde{X}, \tilde{W}, \tilde{Z})$ denote the relatively independent joining of $(X, f(X))$ and (\tilde{W}, \tilde{Z}) over W (with the factor maps given by the natural projections of $(X, f(X))$ onto $f(X) \stackrel{d}{=} W$ and of (\tilde{W}, \tilde{Z}) onto $\tilde{W} \stackrel{d}{=} W$, respectively). Similarly, let $(\tilde{W}, \tilde{Z}, \tilde{Y})$ be the relatively independent joining of (\tilde{W}, \tilde{Z}) and $(g(Y), Y)$ over Z . Now let $(\tilde{X}, \tilde{Y}, \tilde{W}, \tilde{Z})$ be the relatively independent joining of $(\tilde{X}, \tilde{W}, \tilde{Z})$ and $(\tilde{W}, \tilde{Z}, \tilde{Y})$ over (\tilde{W}, \tilde{Z}) . Then the projection of $(\tilde{X}, \tilde{Y}, \tilde{W}, \tilde{Z})$ onto the first two coordinates gives a transition coupling of X and Y with the property that $(f(\tilde{X}), g(\tilde{Y})) \stackrel{d}{=} (\tilde{W}, \tilde{Z})$. We have thus established that every transition coupling (\tilde{W}, \tilde{Z}) of W and Z can be written as $(f(\tilde{X}), g(\tilde{Y}))$ for some transition coupling (\tilde{X}, \tilde{Y}) of X and Y .

The two conclusions of the theorem are immediate consequences of (13) and the result of the previous paragraph. \square

Acknowledgments

KO and ABN were supported in part by NSF grants DMS-1613072 and DMS-1613261. KM gratefully acknowledges the support of NSF CAREER grant DMS-1847144. BY, KM, and ABN would like to acknowledge the support of NSF DMS-2113676.

References

- Abbe, E. (2018) Community detection and stochastic block models: Recent developments. *Journal of Machine Learning Research*, **18**, 1–86. URL <http://jmlr.org/papers/v18/16-480.html>.
- Abbe, E. and Sandon, C. (2015) Community detection in general stochastic block models: Fundamental limits and efficient algorithms for recovery. *2015 IEEE 56th Annual Symposium on Foundations of Computer Science*, 670–688.
- Babai, L. (2015) Graph isomorphism in quasipolynomial time. *ArXiv*, **abs/1512.03547**.
- Barak, B., Chou, C.-N., Lei, Z., Schramm, T. and Sheng, Y. (2019) (Nearly) Efficient Algorithms for the Graph Matching Problem on Correlated Random Graphs. In *NeurIPS*.
- Barbe, A., Sebban, M., Gonçalves, P., Borgnat, P. and Gribonval, R. (2020) Graph diffusion Wasserstein distances. In *European Conference on Machine Learning and Principles and Practice of Knowledge Discovery in Databases*.
- Belkin, M. and Niyogi, P. (2003) Laplacian eigenmaps for dimensionality reduction and data representation. *Neural Computation*, **15**, 1373–1396.
- Blum, A., Hopcroft, J. and Kannan, R. (2020) *Foundations of Data Science*. Cambridge University Press. URL <https://books.google.com/books?id=koHCDwAAQBAJ>.
- Brugere, T., Wan, Z. and Wang, Y. (2023) Distances for markov chains, and their differentiation. *ArXiv*, **abs/2302.08621**. URL <https://api.semanticscholar.org/CorpusID:257020095>.
- Chen, L., Gan, Z., Cheng, Y., Li, L., Carin, L. and Liu, J. (2020) Graph optimal transport for cross-domain alignment. In *International Conference on Machine Learning*, 1542–1553. PMLR.
- Chen, S., Lim, S., Memoli, F., Wan, Z. and Wang, Y. (2022) Weisfeiler-lehman meets gromov-Wasserstein. In *Proceedings of the 39th International Conference on Machine Learning*, Proceedings of Machine Learning Research, 3371–3416. PMLR.
- Chen, S., Lim, S., Memoli, F., Wan, Z. and Wang, Y. (2023) The weisfeiler-lehman distance: Reinterpretation and connection with gnns. *ArXiv*, **abs/2302.00713**.

- Cho, M., Lee, J. and Lee, K. M. (2010) Reweighted random walks for graph matching. In *Computer Vision – ECCV 2010* (eds. K. Daniilidis, P. Maragos and N. Paragios), 492–505. Berlin, Heidelberg: Springer Berlin Heidelberg.
- Cordella, L. P., Foggia, P., Sansone, C. and Vento, M. (2004) A (sub)graph isomorphism algorithm for matching large graphs. *IEEE Transactions on Pattern Analysis and Machine Intelligence*, **26**, 1367–1372.
- Cour, T., Srinivasan, P. and Shi, J. (2007) Balanced graph matching. In *Advances in Neural Information Processing Systems*, vol. 19.
- Cullina, D. and Kiyavash, N. (2017) Exact alignment recovery for correlated Erdos Renyi graphs. *ArXiv*, **abs/1711.06783**.
- Cullina, D., Kiyavash, N., Mittal, P. and Poor, H. V. (2020) Partial Recovery of Erdős-Rényi Graph Alignment via k-Core Alignment. *Abstracts of the 2020 SIGMETRICS/Performance Joint International Conference on Measurement and Modeling of Computer Systems*.
- De La Rue, T. (2005) An introduction to joinings in ergodic theory. *arXiv preprint math/0507429*.
- de la Rue, T. (2009) Joinings in ergodic theory. In *Encyclopedia of Complexity and Systems Science*. Springer, New York, NY.
- Debnath, A. K., Lopez de Compadre, R. L., Debnath, G., Shusterman, A. J. and Hansch, C. (1991) Structure-activity relationship of mutagenic aromatic and heteroaromatic nitro compounds. correlation with molecular orbital energies and hydrophobicity. *Journal of Medicinal Chemistry*, **34**, 786–797.
- Ding, J., Ma, Z., Wu, Y. and Xu, J. (2020) Efficient random graph matching via degree profiles. *Probability Theory and Related Fields*, **179**, 29–115.
- Dong, Y. and Sawin, W. (2020) COPT: Coordinated optimal transport on graphs. In *Advances in Neural Information Processing Systems*.
- Ellis, M. H. (1976) The \bar{d} -distance between two Markov processes cannot always be attained by a Markov joining. *Israel Journal of Mathematics*, **24**, 269–273.
- Ellis, M. H. (1978) Distances between two-state Markov processes attainable by Markov joinings. *Transactions of the American Mathematical Society*, **241**, 129–153.
- Ellis, M. H. (1980) On Kamae’s conjecture concerning the d-distance between two-state Markov processes. *The Annals of Probability*, 372–376.
- Ellis, M. H. *et al.* (1980) Conditions for attaining \bar{d} by a Markovian joining. *The Annals of Probability*, **8**, 431–440.
- Elmsallati, A., Clark, C. and Kalita, J. K. (2016) Global alignment of protein-protein interaction networks: A survey. *IEEE/ACM Transactions on Computational Biology and Bioinformatics*, **13**, 689–705.
- Engel, J., Nardo, M. and Rancan, M. (2021) *Network Analysis for Economics and Finance: An Application to Firm Ownership*, 331–355. Cham: Springer International Publishing.
- Enqvist, O., Josephson, K. and Kahl, F. (2009) Optimal correspondences from pairwise constraints. In *2009 IEEE 12th International Conference on Computer Vision*, 1295–1302.
- Fagiolo, G., Reyes, J. and Schiavo, S. (2010) The evolution of the world trade web: a weighted-network analysis. *Journal of Evolutionary Economics*, **20**, 479–514.
- Feizi, S., Quon, G. T., Recamonde-Mendoza, M., Médard, M., Kellis, M. and Jadbabaie, A. (2020) Spectral alignment of graphs. *IEEE Transactions on Network Science and Engineering*, **7**, 1182–1197.
- Furstenberg, H. (1967) Disjointness in ergodic theory, minimal sets, and a problem in diophantine approximation. *Theory of Computing Systems*, **1**, 1–49.
- Garey, M. R. and Johnson, D. S. (1990) *Computers and Intractability; A Guide to the Theory of NP-Completeness*. W. H. Freeman & Co.
- Glasner, E. (2003) *Ergodic Theory via Joinings*, vol. 101. American Mathematical Society.

- Gold, S. and Rangarajan, A. (1996) A graduated assignment algorithm for graph matching. *IEEE Transactions on Pattern Analysis and Machine Intelligence*, **18**, 377 – 388.
- Gray, R. M., Neuhoff, D. L. and Shields, P. C. (1975) A generalization of Ornstein’s \bar{d} distance with applications to information theory. *The Annals of Probability*, 315–328.
- Grover, A. and Leskovec, J. (2016) node2vec: Scalable feature learning for networks. *Proceedings of the 22nd ACM SIGKDD International Conference on Knowledge Discovery and Data Mining*.
- Hamilton, W. L. (2020) Graph representation learning. *Synthesis Lectures on Artificial Intelligence and Machine Learning*, **14**, 1–159.
- Holland, P. W., Laskey, K. B. and Leinhardt, S. (1983) Stochastic blockmodels: First steps. *Social Networks*, **5**, 109–137.
- Howard, R. A. (1960) *Dynamic Programming and Markov Processes*. John Wiley.
- Jackson, G. L., Kennedy, D., Bradbury, T. N. and Karney, B. R. (2014) A social network comparison of low-income black and white newlywed couples. *Journal of Marriage and Family*, **76**, 967–982.
- Jiang, B., Tang, J., Ding, C., Gong, Y. and Luo, B. (2017) Graph matching via multiplicative update algorithm. In *Advances in Neural Information Processing Systems*, vol. 30.
- Kalaev, M., Bafna, V. and Sharan, R. (2008) Fast and accurate alignment of multiple protein networks. *Journal of computational biology : a journal of computational molecular cell biology*, **16 8**, 989–99.
- Kelley, B. P., Sharan, R., Karp, R. M., Sittler, T., Root, D. E., Stockwell, B. R. and Ideker, T. (2003) Conserved pathways within bacteria and yeast as revealed by global protein network alignment. *Proceedings of the National Academy of Sciences of the United States of America*, **100**, 11394 – 11399.
- Kersting, K., Kriege, N. M., Morris, C., Mutzel, P. and Neumann, M. (2016) Benchmark data sets for graph kernels. <http://graphkernels.cs.tu-dortmund.de>.
- Klau, G. W. (2009) A new graph-based method for pairwise global network alignment. *BMC Bioinformatics*, **10**, S59 – S59.
- Korula, N. and Lattanzi, S. (2014) An efficient reconciliation algorithm for social networks. *ArXiv*, **abs/1307.1690**.
- Kriege, N. M., Fey, M., Fisseler, D., Mutzel, P. and Weichert, F. (2018) Recognizing Cuneiform signs using graph based methods. In *International Workshop on Cost-Sensitive Learning*, 31–44. PMLR.
- Kuchaiev, O., Milenković, T., Memisevic, V., Hayes, W. B. and Przulj, N. (2010) Topological network alignment uncovers biological function and phylogeny. *Journal of The Royal Society Interface*, **7**, 1341 – 1354.
- Kuchaiev, O. and Przulj, N. (2011) Integrative network alignment reveals large regions of global network similarity in yeast and human. *Bioinformatics*, **27 10**, 1390–6.
- Lassalle, R. (2013) Causal transport plans and their monge–kantorovich problems. *Stochastic Analysis and Applications*, **36**, 452 – 484.
- Lee, C. and Wilkinson, D. (2019) A review of stochastic block models and extensions for graph clustering. *Applied Network Science*, **4**, 1–50.
- Liordeanu, M. and Hebert, M. (2005) A spectral technique for correspondence problems using pairwise constraints. In *IEEE International Conference on Computer Vision*, vol. 2, 1482–1489 Vol. 2.
- Liordeanu, M., Hebert, M. and Sukthankar, R. (2009) An integer projected fixed point method for graph matching and map inference. In *Advances in Neural Information Processing Systems*, vol. 22.
- Levin, D. A. and Peres, Y. (2017) *Markov Chains and Mixing Times*, vol. 107. American Mathematical Soc.
- Lind, D. and Marcus, B. (1995) *An Introduction to Symbolic Dynamics and Coding*. Cambridge University Press.

- Loiola, E., Abreu, N., Boaventura-Netto, P., Hahn, P. and Querido, T. (2007) A survey of the quadratic assignment problem. *European Journal of Operational Research*, **176**, 657–690.
- Lyzinski, V., Fishkind, D. E. and Priebe, C. E. (2014) Seeded graph matching for correlated Erdős-Rényi graphs. *J. Mach. Learn. Res.*, **15**, 3513–3540.
- Ma, C.-Y. and Liao, C.-S. (2020) A review of protein–protein interaction network alignment: From pathway comparison to global alignment. *Computational and Structural Biotechnology Journal*, **18**, 2647–2656.
- Maretic, H. P., Gheche, M. E., Chierchia, G. and Frossard, P. (2019) GOT: An Optimal Transport framework for Graph comparison. In *Advances in Neural Information Processing Systems*.
- Maretic, H. P., Gheche, M. E., Minder, M., Chierchia, G. and Frossard, P. (2020) Wasserstein-based graph alignment. *arXiv preprint arXiv:2003.06048*.
- McKay, B. D. and Piperno, A. (2014) Practical graph isomorphism, ii. *J. Symb. Comput.*, **60**, 94–112.
- Mémoli, F. (2011) Gromov–Wasserstein distances and the metric approach to object matching. *Foundations of Computational Mathematics*, **11**, 417–487.
- Milano, M., Guzzi, P. H., Tymofiyeva, O., Xu, D., Hess, C. P., Veltri, P. and Cannataro, M. (2017) An extensive assessment of network alignment algorithms for comparison of brain connectomes. *BMC Bioinformatics*, **18**.
- Mislove, A., Marcon, M., Gummadi, K. P., Druschel, P. and Bhattacharjee, B. (2007) Measurement and analysis of online social networks. In *Proceedings of the 7th ACM SIGCOMM conference on Internet measurement*, 29–42.
- O’Connor, K., McGoff, K. and Nobel, A. B. (2021) Estimation of stationary optimal transport plans. *arXiv preprint arXiv:2107.11858*.
- O’Connor, K., McGoff, K. and Nobel, A. B. (2022) Optimal transport for stationary Markov chains via policy iteration. *Journal of Machine Learning Research*, **23**, 1–52.
- Ornstein, D. S. (1973) An application of ergodic theory to probability theory. *The Annals of Probability*, **1**, 43–58.
- Perozzi, B., Al-Rfou, R. and Skiena, S. (2014) DeepWalk: online learning of social representations. *Proceedings of the 20th ACM SIGKDD international conference on Knowledge discovery and data mining*.
- Peyré, G. and Cuturi, M. (2019) *Computational Optimal Transport*. Now Publishers, Inc.
- Peyré, G., Cuturi, M. and Solomon, J. (2016) Gromov-Wasserstein averaging of kernel and distance matrices. In *International Conference on Machine Learning*, 2664–2672. PMLR.
- Plummer, M. D. (2007) Graph factors and factorization: 1985–2003: a survey. *Discrete Mathematics*, **307**, 791–821.
- Riesen, K. and Bunke, H. (2008) IAM graph database repository for graph based pattern recognition and machine learning. In *Joint International Workshops on Statistical Techniques in Pattern Recognition and Structural and Syntactic Pattern Recognition*, 287–297. Springer.
- Schellewald, C. and Schnörr, C. (2005) Probabilistic subgraph matching based on convex relaxation. In *Energy Minimization Methods in Computer Vision and Pattern Recognition*, 171–186. Berlin, Heidelberg: Springer Berlin Heidelberg.
- Singh, R., Xu, J. and Berger, B. (2008) Global alignment of multiple protein interaction networks with application to functional orthology detection. *Proceedings of the National Academy of Sciences*, **105**, 12763–12768.
- Song, J., Gao, Y., Wang, H. and An, B. (2016) Measuring the distance between finite Markov decision processes. In *Proceedings of the 2016 international conference on autonomous agents & multiagent systems*, 468–476. International Foundation for Autonomous Agents and Multiagent Systems.
- Sutherland, J. J., O’Brien, L. A. and Weaver, D. F. (2003) Spline-fitting with a genetic algorithm: A method for developing classification structure- activity relationships. *Journal of Chemical Information and Computer Sciences*, **43**, 1906–1915.

- Titouan, V., Courty, N., Tavenard, R. and Flamary, R. (2019) Optimal transport for structured data with application on graphs. In *International Conference on Machine Learning*, 6275–6284.
- Toivonen, H., Zhou, F., Hartikainen, A. and Hinkka, A. (2011) Compression of weighted graphs. In *International Conference on Knowledge Discovery and Data Mining*, 965–973.
- Torr, P. H. S. (2003) Solving Markov Random Fields using Semi Definite Programming. *AI & Society*.
- van Wyk, B. and van Wyk, M. (2004) A POCS-based graph matching algorithm. *IEEE Transactions on Pattern Analysis and Machine Intelligence*, **26**, 1526–1530.
- Vayer, T., Chapel, L., Flamary, R., Tavenard, R. and Courty, N. (2020) Fused Gromov-Wasserstein distance for structured objects. *Algorithms*, **13**, 212.
- Vayer, T., Flamary, R., Tavenard, R., Chapel, L. and Courty, N. (2019) Sliced Gromov-Wasserstein. In *Advances in Neural Information Processing Systems*.
- Villani, C. (2008) *Optimal Transport: Old and New*, vol. 338. Springer-Verlag Berlin Heidelberg.
- Vishwanathan, S., Schraudolph, N. N., Kondor, R. and Borgwardt, K. M. (2010) Graph kernels. *Journal of Machine Learning Research*, **11**, 1201–1242.
- Xu, H., Luo, D. and Carin, L. (2019a) Scalable Gromov-Wasserstein learning for graph partitioning and matching. In *Advances in Neural Information Processing Systems*, 3052–3062.
- Xu, H., Luo, D., Zha, H. and Duke, L. C. (2019b) Gromov-Wasserstein learning for graph matching and node embedding. In *International Conference on Machine Learning*, 6932–6941.
- Yan, J., Yin, X.-C., Lin, W., Deng, C., Zha, H. and Yang, X. (2016) A short survey of recent advances in graph matching. In *Proceedings of the 2016 ACM on International Conference on Multimedia Retrieval*, 167–174. New York, NY, USA: Association for Computing Machinery. URL <https://doi.org/10.1145/2911996.2912035>.
- Yan, X., Cheng, H., Han, J. and Yu, P. S. (2008) Mining significant graph patterns by leap search. In *SIGMOD Conference*.
- Yartseva, L. and Grossglauser, M. (2013) On the performance of percolation graph matching. In *COSN '13*.
- Yu, T., Yan, J., Wang, Y., Liu, W. and Li, b. (2018) Generalizing graph matching beyond quadratic assignment model. In *Advances in Neural Information Processing Systems*, vol. 31. Curran Associates, Inc.
- Zalesky, A., Fornito, A. and Bullmore, E. T. (2010) Network-based statistic: identifying differences in brain networks. *Neuroimage*, **53**, 1197–1207.
- Zaslavskiy, M., Bach, F. and Vert, J.-P. (2009) A Path Following Algorithm for the Graph Matching Problem. *IEEE Transactions on Pattern Analysis and Machine Intelligence*, **31**, 2227–2242.
- Zhang, S. (2000) Existence and application of optimal Markovian coupling with respect to non-negative lower semi-continuous functions. *Acta Mathematica Sinica*, **16**, 261–270.
- Zhou, F. and De la Torre, F. (2016) Factorized graph matching. *IEEE Transactions on Pattern Analysis and Machine Intelligence*, **38**, 1774–1789.

Appendix A Experimental Details

In this appendix, we provide further details for the experiments discussed in Section 6. We refer to `ExactOTC` as the exact implementation of NetOTC, while `EntropicOTC` specifically represents the regularized version of the NetOTC algorithm.

A.1 Network Classification

In order to compute approximate solutions to the NetOTC problem, we used the `EntropicOTC` algorithm with $L = 10$, $T = 50$, $\xi = 100$, and 50 Sinkhorn iterations. The FGW cost was computed with a default parameter choice of $\alpha = 0.5$. The experiment was run on Matlab and a 24-core node in a university-owned computing cluster.

A.2 Network Isomorphism

The classes of networks we dealt with in this experiment are as follows. We give details on how we generated the random networks.

- **SBM:** A description of an SBM is provided in Section 6.4. The given set informs the number of vertices in each block. For example, `SBM(7,7,7)` indicates an SBM having 4 blocks with 7 vertices in each block. `SBM(10,8,6)` has 3 blocks, and each block has 10, 8, and 6 vertices. The connection probabilities within the block were fixed to 0.7, and the probabilities between blocks were 0.1.
- **Erdos-Renyi network:** Erdos-Renyi network is a random network in which every pair of vertices is connected with an independent probability p by an unweighted edge. Remark that the Erdos-Renyi network is equivalent to an SBM with a single block. For each network generation, the number of vertices was randomly determined from the given set. The connection probability p was fixed as given in each class.
- **Random weighted adjacency matrix:** Each element of the adjacency matrix is randomly sampled from the given set. For example, random weighted adjacency matrix $\{0, 1, 2\}$ indicates a network that its adjacency matrix elements are all sampled from the set $\{0, 1, 2\}$. In order to restrict the network to an undirected network, we only sample the upper triangular matrix and the lower triangular matrix is symmetrically filled. Note that the number of vertices is randomly determined between 6 and 20.
- **Random Lollipop network:** An example of a lollipop network is presented in Figure 5. A lollipop consists of a candy part and a stick part. The number of vertices in the candy part is randomly chosen between 7 and 15. The number of vertices in the stick part is also determined between 7 and 15. We also add edges inside the candy to vary the lollipop. With a probability of 0.5, we connect an edge between pair of vertices in the candy.

We discuss how we establish if the algorithm successfully identified the isomorphism map. For given two isomorphic networks $G_1 = (U, E_1, w_1)$ and $G_2 = (V, E_2, w_2)$, each algorithm returns an vertex alignment $\pi_v : (U, V) \rightarrow [0, 1]$. Define a hard alignment function $\psi(\cdot) = \operatorname{argmax}_{v \in V} \pi(\cdot, v)$, where $\psi : U \rightarrow V$ returns the most aligned vertex in G_2 for each vertex in G_1 . If ψ satisfies the following conditions, the algorithm correctly detects the isomorphism.

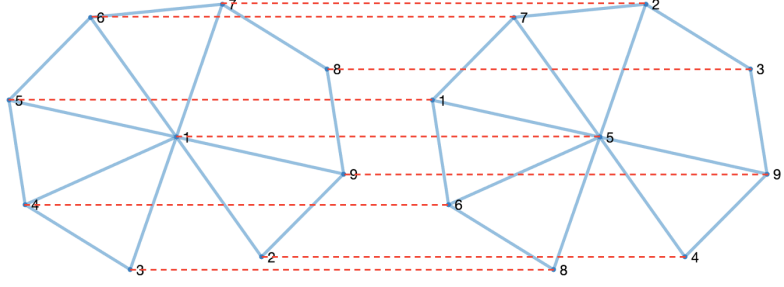
1. ψ is bijective.
2. For every $(u_1, u_2) \in E_1$, $(\psi(u_1), \psi(u_2)) \in E_2$ and $w_2(\psi(u_1), \psi(u_2)) = w_1(u_1, u_2)$.
3. For every $(v_1, v_2) \in E_2$, $(\psi^{-1}(v_1), \psi^{-1}(v_2)) \in E_1$ and $w_1(\psi^{-1}(v_1), \psi^{-1}(v_2)) = w_2(v_1, v_2)$.

Figure 8 shows an additional example of detecting network isomorphism. As in Figure 5, NetOTC successfully detects isomorphism, while OT and FGW do not.

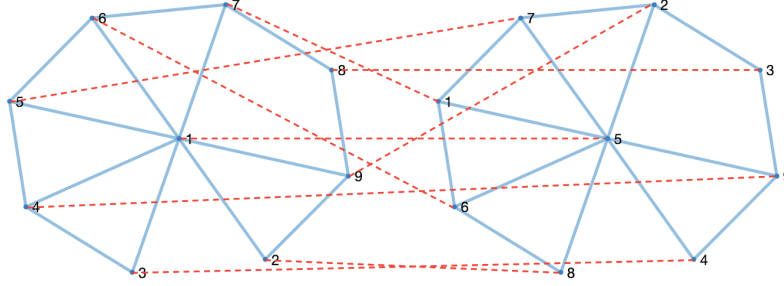
The `ExactOTC` algorithm was utilized to solve the NetOTC problem, and a fixed $\alpha = 0.5$ was used for FGW. Note that the algorithms were applied only to the connected network among the generated networks. 95.48% of the generated networks were connected on average. The experiment was developed in Matlab and run on a 24-core node in a university-owned computing cluster.

A.3 Stochastic Block Model Alignment

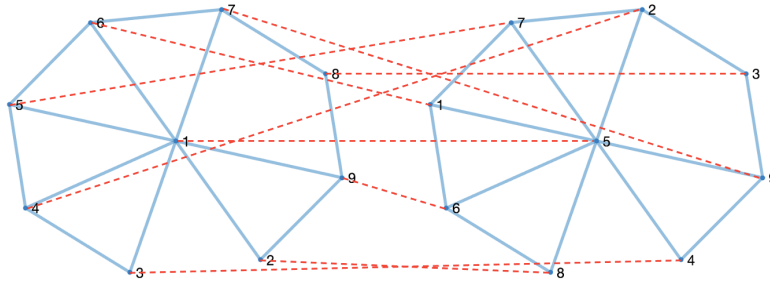
Cross validation was performed for FGW (to select $\alpha \in \{0, 0.1, \dots, 1\}$) by randomly generating 10 pairs of SBM networks and computing alignments of vertices and edges. Parameters that yielded the highest average alignment accuracy were selected, where separate parameters were chosen for optimizing vertex and edge alignment.



(a) NetOTC alignment.



(b) OT alignment.



(c) FGW alignment.

Figure 8: Alignment of two isomorphic wheel networks obtained by NetOTC, OT, and FGW. To make the task challenging, two edges were removed.

0.1 and 1 were selected for vertex and edge alignment, respectively. We note that this implies GW and FGW were equivalent for edge alignment in our experiment. The `ExactOTC` algorithm was used to compute solutions to the NetOTC problem. The experiment was developed and run in Matlab on a personal machine.

A.4 Network Factors

Network G_2 has b vertices embedded in \mathbb{R}^5 where the vertices are sampled from $\mathcal{N}_5(0, \sigma^2 \mathbf{I}_5)$. We denote the vertices of G_2 as V_1, \dots, V_b . Then, we sample m points from $\mathcal{N}_5(V_i, \mathbf{I}_5)$ for each $i = 1, \dots, b$ and the points will be the vertices of G_1 . The total number of vertices of G_1 is bm . We set $b = 6$ and $m = 5$ in this experiment. We used $\alpha = 0.5$ as a default trade-off parameter when applying FGW. We note that the choice of $\alpha \in \{0, 0.1, \dots, 1\}$ doesn't affect the alignment result much.

This experiment was conducted not only in exact factor situations but also when we have approximate factors. We call it an approximate factor when Definition 12 approximately holds as follows. For every $v, v' \in V$ and a given error rate $\epsilon > 0$,

$$\sum_{u' \in f^{-1}(v')} w_1(u, u') \in \left[(1 - \epsilon) \frac{d_1(u)}{d_2(v)} w_2(v, v'), (1 + \epsilon) \frac{d_1(u)}{d_2(v)} w_2(v, v') \right], \quad \forall u \in f^{-1}(v),$$

and

$$\sum_{u \in f^{-1}(v)} \sum_{u' \in f^{-1}(v')} w_1(u, u') = \sum_{u \in f^{-1}(v)} \frac{d_1(u)}{d_2(v)} w_2(v, v').$$

	Exact factor	Approximate factor
	NetOTC	NetOTC
$\sigma = 2.5$	100.00 \pm 0.00	97.94 \pm 0.26
$\sigma = 2.0$	99.91 \pm 0.65	97.57 \pm 1.03
$\sigma = 1.5$	97.46 \pm 4.84	95.87 \pm 3.37
$\sigma = 1.0$	84.09 \pm 11.02	84.06 \pm 11.07

Table 5: Directed networks: alignment accuracies of network factors. Average accuracies observed over 100 random network factors are reported along with their standard deviation.

	AIDS	BZR	Cuneiform	MCF-7	MOLT-4	MUTAG	Yeast
# of Vertices	13.25	34.65	20.2	26.65	26.7	17.9	20.43
ExactOTC	4.35	37.83	10.52	22.78	24.47	9.12	10.82
EntropicOTC	0.43	5.57	1.04	2.91	3.07	0.77	1.12

Table 6: Average Runtimes for datasets investigated in Section 6.2 (sec). We also report the average number of vertices for the randomly selected 20 pairs of graphs.

	ExactOTC	EntropicOTC
SBM-48-32	41.92	6.26
SBM-96-64	334.53	156.58
SBM-128-96	2143.42	1042.46

Table 7: Runtimes for pairs of SBM (sec). SBM- a - b denotes a comparison of two SBMs with a total of a vertices and b vertices.

In particular, we allowed 5% error ($\epsilon = 0.05$) for the second condition in this experiment.

Table 5 reports the vertex alignment accuracy of NetOTC for directed networks at various variance settings. We may check that the performances are similar to applying NetOTC to undirected factor network pairs. Similar to the Stochastic Block Model Alignment experiment, the ExactOTC algorithm was used to obtain solutions to the NetOTC problem and was run in Matlab on a personal machine.

A.5 Runtime Analysis of NetOTC

We report the runtime of NetOTC for the experiments discussed in Sections 6.2 and 6.4. The runtime metrics are presented for both ExactOTC and EntropicOTC, employing our Matlab implementation of these methods. First, we randomly selected 20 pairs of graphs from each of the seven datasets used in Section 6.2. The average computation time for each pair is detailed in Table 6. Next, we investigated the computation time for comparing two stochastic block models (SBMs). Following the procedure detailed in Section 6.4, we generated SBMs with 4 blocks. The within-block connection probabilities were set to 1, 0.8, 0.6, and 0.4, while the between-block connection probability was fixed at 0.1. The runtime results for comparing these SBMs are presented in Table 7.